

N72-23797

APOLLO CRYOGENIC INTEGRATED SYSTEMS PROGRAM

R. K. M. Seto

J. E. Cunningham

TRW SYSTEMS GROUP

HOUSTON, TEXAS

ACKNOWLEDGEMENTS

The development of the Apollo Cryogenic Storage System Integrated Systems Program was the result of the combined efforts of several individuals. The contributions of these individuals are acknowledged.

The tankage model was developed by C. E. Barton. J. G. Torian and R. A. Cailleateau developed the components and lines model. The vehicle thermal model was derived by P. J. Knowles, while the oxygen and hydrogen thermophysical routines were adapted by E. Joseph. Programmers for the effort were J. G. Lindsey, J. I. Prewitt and A. Rios.

ABSTRACT

The Integrated Systems Program is capable of simulating both nominal and anomalous operation of the Apollo Cryogenics Storage System (CSS). Two versions of the program exist; one for the Apollo 14 configuration and the other for "J" Type Mission configurations. The program consists of two mathematical models which are dynamically coupled. A model of the CSS components and lines determines the oxygen and hydrogen flowrate from each storage tank given the tank pressures and temperatures, and the Electrical Power Subsystem (EPS) and Environmental Control Subsystem (ECS) flow demands. Temperatures and pressures throughout the components and lines are also determined. A model of the CSS tankage determines the pressure and temperatures in the tanks given the flowrate from each tank and the thermal environment. The model accounts for tank stretch and includes simplified oxygen tank heater and stratification routines. Supporting subroutines are used to calculate thermophysical properties from National Bureau of Standards (NBS) data and to calculate the CSS thermal environment during various mission phases. Anomalous conditions such as a fan and/or heater failure, degraded tank vacuum annulus performance, failed check valves, and leaking lines can be simulated. The program is currently operational on the Univac 1108 computer.

CONTENTS

| | Page |
|---|------|
| ABSTRACT..... | 333 |
| TABLE OF CONTENTS..... | 334 |
| INTRODUCTION..... | 336 |
| SYSTEM DESCRIPTION..... | 338 |
| Cryogenic Storage Tanks..... | 338 |
| Cryogenic System Components and Lines..... | 339 |
| ANALYTICAL FORMULATION..... | 342 |
| Storage Tank Model..... | 342 |
| Oxygen Tanks..... | 343 |
| Hydrogen Tanks..... | 345 |
| Component and Line Model..... | 346 |
| Matrix Model..... | 346 |
| Nodal Model..... | 347 |
| Lines and Fittings..... | 347 |
| Filters, Check Valves, Relief Valves and Shutoff Valves..... | 348 |
| Restrictors..... | 348 |
| Overboard Vents..... | 348 |
| Auxiliary Routines..... | 349 |
| Vehicle Thermal Model..... | 349 |
| Oxygen Tank Heat Leak..... | 349 |
| Hydrogen Tank Heat Leak..... | 351 |
| Vacuum Annulus Failure..... | 351 |
| Component and Line Environmental Temperatures..... | 352 |
| Thermophysical Properties of Oxygen and Hydrogen..... | 352 |
| Oxygen Properties..... | 353 |
| Hydrogen Properties..... | 355 |
| REFERENCES..... | 356 |
| APPENDIX I - NOMENCLATURE..... | 389 |
| APPENDIX II - DERIVATION OF THE RATE OF PRESSURE CHANGE IN THE CSS TANKS..... | 393 |
| APPENDIX III - DERIVATION OF EQUATIONS USED IN THE COMPONENT AND LINE MODEL..... | 404 |

TABLES

| | |
|---|-----|
| 1. Cryogenic System Operational Parameters..... | 357 |
| 2. Curve Fit Coefficients Representative of the CSS Thermal Environment..... | 359 |
| 3. Environmental Temperature Locations..... | 362 |
| 4. Constants for Stewart's Equation of State..... | 363 |
| 5. Variables for Computing Isotherm Derivatives..... | 364 |
| 6. Variables for Computing Isochor Derivatives..... | 365 |
| 7. Thermophysical Properties Subroutines..... | 366 |

CONTENTS (Continued)

| | Page |
|-------------------------------------|------|
| A-1. Cryogenic Tank Properties..... | 402 |

FIGURES

| | |
|---|-----|
| 1. SM Sector IV CSS Tankage Arrangement..... | 368 |
| 2. SM Sector I CSS Tankage Arrangement..... | 369 |
| 3. Apollo 14 Cryogenic Storage System Oxygen Schematic..... | 370 |
| 4. Apollo 14 Cryogenic Storage System Hydrogen Schematic..... | 371 |
| 5. Apollo J Type Cryogenic Storage System Oxygen Schematic..... | 372 |
| 6. Apollo J Type Cryogenic Storage System Hydrogen Schematic..... | 373 |
| 7. Integrated Systems Program Flow Diagram..... | 374 |
| 8. Storage Tank Model Flow Diagram..... | 375 |
| 9. Oxygen Tank Nodal Model..... | 376 |
| 10. Component and Line Model Flow Diagram..... | 377 |
| 11. Electrical Analog of the Oxygen System for the Matrix Model... | 378 |
| 12. Electrical Analog of the Hydrogen System for the Matrix Model. | 379 |
| 13. Electrical Analog of the Oxygen System for the Nodal Model.... | 380 |
| 14. Electrical Analog of the Hydrogen System for the Nodal Model.. | 382 |
| 15. Equivalent L/D for Bend Losses..... | 383 |
| 16. Check Valve Resistance Characteristics..... | 384 |
| 17. Relief Valve Resistance Characteristics..... | 384 |
| 18. Restrictor Pressure Drop..... | 385 |
| 19. Hydrogen Tank Heat Leak..... | 386 |
| 20. Variation in Heat Leak for the CSS Tanks for Loss of Vacuum in the Annulus-Air Leakage..... | 388 |
| 21. Variation in Heat Leak for the CSS Tanks for Loss of Vacuum in the Annulus-Hydrogen or Oxygen Leakage..... | 389 |

INTRODUCTION

The Integrated Systems Program is a mathematical representation of the Apollo Cryogenic Storage System (CSS) and is capable of simulating both nominal and anomalous operation of the system. The program is modular in structure and consists of a storage tank model, a components and lines model and auxiliary routines. Two versions of the program exist; one for the Apollo 14 spacecraft configuration and the other for the "J" Type Mission configuration. The "J" configuration differs from the Apollo 14 configuration primarily by the addition of a hydrogen storage tank and several other components.

The tankage model is capable of simulating the thermodynamic performance of the CSS hydrogen and oxygen tanks. The model accounts for the effects of heat leakage, heater and/or fan operation, duty cycles, and control equipment as well as all significant thermal, elastic, thermoelastic and thermodynamic effects which influence tank performance. Capability to predict the effects of thermal stratification on the oxygen tank performance and to define oxygen tank heater temperatures are included.

The components and lines model determines the oxygen and hydrogen flowrate from each storage tank based on the pressures and temperatures of the individual tanks and the flow demands of the Electrical Power Subsystem (EPS) and the Environmental Control Subsystem (ECS). A transient analysis is performed to determine the pressures and temperatures at each junction and the flowrates in each leg of the system. These values are used to determine the instantaneous steady state pressure drop across all components in each leg.

Anomalous operation of the tanks, such as heater and/or fan failures, degraded tank vacuum annulus performance, and loss of tanks, may be simulated. In addition, line leaks and anomalous operation of any component may be simulated for the oxygen and/or hydrogen distribution systems.

The auxiliary routines describe the thermal environment of the CSS and provide oxygen and hydrogen thermophysical data. The vehicle thermal model computes the outer wall temperatures of the storage tanks as well as spacecraft bay wall and shelf temperatures for various mission phases including translunar coast, transearth coast, attitude holds, and lunar orbit. The thermophysical data routine contains data for both oxygen and hydrogen obtained from the National Bureau of Standards (NBS) over the expected system operating range.

Input to the Integrated Systems program includes the initial state and quantities of the cryogens in the tanks, EPS and ECS flowrate demands, component characteristics, inertial accelerations and the mission mode.

The program, written in Fortran V, is operational on the Univac 1108 computer.

SYSTEM DESCRIPTION

The Apollo CSS supplies oxygen and hydrogen on a demand basis to the EPS and the ECS. The cryogenic fluids are stored in their supercritical states in tanks located in the Service Module (SM). Each tank is equipped with individual components for filling; venting; quantity, temperature, and pressure measurements; pressure control and relief; and the accompanying displays and controls. For all missions through Apollo 13, the storage system was comprised of two hydrogen tanks and two oxygen tanks. The arrangement of these tanks in Sector IV of the SM is shown in Figure 1. For the Apollo 14 Mission the storage system consisted of an additional oxygen tank located in Sector I of the SM making a total of three oxygen tanks and two hydrogen tanks. Subsequent missions will have three hydrogen tanks as well as three oxygen tanks. The additional hydrogen tank will also be located in Sector I of the SM. Figure 2 presents the tankage arrangement in Sector I.

During nominal operation, the storage system is maintained at a relatively constant pressure with fluid temperature increasing during the mission. Pressure is maintained above the critical pressure in the tanks by the application, either manually or automatically, of electrical heater power. Prior to the Apollo 14 Mission, electrical heat was supplied to the storage tanks in conjunction with destratification fans. However, subsequent to the Apollo 13 oxygen system failure, the system was redesigned to eliminate the fans in the oxygen tanks, although fans are still used in the hydrogen tanks.

The nominal operating pressure of the storage tanks is 245 ± 15 psia and 900 ± 35 psia for the hydrogen and oxygen tanks, respectively.

The fluid flow rate is controlled on a demand basis by the ECS and EPS regardless of the storage system's pressure or operating mode. Under nominal operating conditions there are 29.3 pounds of hydrogen and 330.1 pounds of oxygen loaded into each of the storage tanks. Of these amounts, there are 28.2 pounds of usable hydrogen and 323.5 pounds of usable oxygen. Other pertinent storage system operational parameters are presented in Table 1.

Cryogenic Storage Tanks

A major difference between the oxygen and hydrogen tanks is in the material used in their fabrication. These materials are listed in Table 1 and were obtained from Reference 1. In the broad sense, the

physical configuration for both tanks is similar in nature and they can be described as a typical unit.

Each tank consists of two concentric spherical shells with thermal insulation in the annular space between the shells. In the oxygen tanks, the insulation supports the pressure vessel. The annulus of each tank is equipped with a vac-ion pump to maintain the low pressure required for adequate vacuum insulation, although in flight the oxygen pumps are the only pumps which may be operated. In addition, the pressure vessel supports (hydrogen tank only), fluid lines, and the electrical conduit are located within the evacuated annulus. The exit fluid line is routed through the annulus before exiting from the tank to provide vapor cooling.

Prior to Apollo 13, each tank was equipped with a two element heater and two destratification fans. However, following the Apollo 13 oxygen system failure, the two element heater and destratification fans in the oxygen tanks were removed and replaced with a three element heater. In addition, the heater thermostat for protection against high heater temperatures was removed and replaced with a temperature sensor. The new sensor is located on the heater tube. Another temperature sensor is located above the capacitance probe and measures the bulk fluid temperature. Electrical lines leading into the redesigned oxygen tank have also been sheathed to reduce the fire hazard.

Cryogenic System Components and Lines

Figures 3 and 4 are schematics of the component and line configurations for the Apollo 14 oxygen and hydrogen systems, respectively, showing the relative locations of the components which make up the system. Figures 5 and 6 present similar schematics for the "J" Type Mission system. In general, the system is composed of lines, valve modules, flow filters and flow restrictors. For missions prior to Apollo 14, the system valve modules for both the hydrogen and oxygen systems each contained two relief valves, two pressure transducers, two pressure switches and one check valve. For Apollo 14, a half valve module was added for oxygen tank 3 and contains one relief valve, one pressure switch, and a check valve. A solenoid operated shutoff valve was also added between oxygen tanks 2 and 3.

The relief valves in these modules are a gradual opening differential pressure poppet type which assures the lowest possible leakage with virtually zero delta pressure between crack and full flow. These valves are designed to be unaffected by back pressure in the downstream plumbing and are temperature compensated over the full range of fluid temperatures which may occur.

The pressure transducers are absolute pressure devices which utilize bonded strain gauges to produce millivolt signals to the signal conditioner. The signal conditioner is integral to the transducer with a 0 to 5 VDC output linearly proportioned to tank pressure. The transducers can operate at environmental temperatures as low as -80°F and are capable of supplying a continuous readout of pressure over the specified range with a maximum error of $\pm 2\text{-}1/2$ percent of full scale.

The pressure switches are single-throw, single pole absolute pressure devices which may be used to control the motor switches which activate the destratification motors and/or tank heaters. These switches have been used successfully in an environment of -400°F .

The check valve is a spring loaded poppet type and is designed to open at a differential pressure of approximately 1 psi. The valve seat has a large area to prevent chattering during flow in the normal direction and to help obtain a positive seal if pressurized in the reverse direction.

The fuel cell valve module for the hydrogen system consists of two check valves and three solenoid operated valves in one valve body. The check valves are a dual seat type which allow the main passage to be full open and the auxiliary passage barely cracked at low flows. At high flows, both the main and auxiliary passages are completely open. The solenoid valves are poppet latch type and are actuated by a magnetic armature suspended on a Bellville spring. Opening and closing coils on both sides of the armature actuate the valve. The valves open against pressure and pressure helps to seal the valve against leakage when closed to flow in the normal flow direction.

For the oxygen system, the fuel cell valve module contains check valves similar to those in the hydrogen fuel cell valve module. However, subsequent to Apollo 13, the solenoid valves have been taken out of the module and mounted externally and upstream of the flow transducers to the fuel cells.

The oxygen and hydrogen inline filters consist of several chemically etched discs stacked in a cartridge. They are rated at 5 microns nominally and 12 microns absolute with a capacity to contain .25 grams contaminant.

Several components have been added to the CSS for missions subsequent to the Apollo 14 ("J" type missions). A half valve module containing a relief valve, a pressure switch, and a check valve has been added for the third hydrogen tank. There are three oxygen restrictors in the ECS for "J" type missions versus two for other Apollo missions. The third restrictor line is a branch of the oxygen tank 2 ECS supply line and reconnects downstream of the junction of the other two restrictor lines. This restrictor line includes a filter and check valve.

ANALYTICAL FORMULATION

The Integrated Systems Program was developed as a tool to aid in the preflight planning and the postflight analysis of the Apollo Cryogenic Storage System. Modular in structure, the program is comprised of a tankage model, a components and line model and several auxiliary subroutines. All significant effects which influence system performance, such as thermal environment and mission mode, are included.

Given the component characteristics, the initial state of the cryogens in the tanks, the EPS and ECS flow requirements and the mission mode, the program is capable of simulating the nominal performance of the CSS. Figure 7 presents a flow diagram of the program. Output includes the temperature, pressure and flowrates at various points in the system as well as the remaining quantities and state of the cryogens in the tanks.

In addition to nominal performance, the program is capable of simulating the operation of the CSS under anomalous conditions. The effects of degraded performance of the tank vacuum annulus caused by the presence of air or the cryogen in the jacket may be determined. Abnormal environmental temperatures or tank fan and heater failures may be simulated. Anomalous operation of the check valves, filters, relief valves or flow restrictors may be investigated. Oxygen or hydrogen line leaks may be modeled nearly anywhere in the system.

Two versions of the program were developed. One version is capable of simulating the CSS up to and including the Apollo 14 configuration. The other is capable of simulating the "J" Type Mission configuration. The primary difference in these programs is in the components and lines model. Only the "J" Type configuration will be discussed in this document.

The following sections discuss the analytical formulation of the major models and supporting subroutines which comprise the Integrated Systems Program.

Storage Tank Model

The storage tank model was developed to simulate the thermodynamic performance of the Apollo CSS oxygen and hydrogen tanks. Given the initial conditions and flow demands, the model simultaneously updates the thermodynamic state in each storage tank based on control equipment operation, tank characteristics and heat leak. A flow diagram of the

model is presented in Figure 8.

The model may be divided into two sections. The first section determines the maximum time increment over which all tanks may be simulated. The second section uses this time increment to update the state of the fluid in each tank corresponding with the conditions which prevail at the end of the time increment.

The time increment depends on the rate of change of pressure and the operation of the pressure switches in each tank. The time for the tank pressure to reach a specified excursion (currently 15 psi) from its initial state is compared to the time required to reach the pressure control limit. The shorter of these two time intervals is defined as the maximum dynamic simulation time increment for a given tank. Dynamic simulation time increments for all tanks are compared and the smallest one is chosen as the total tank system dynamic simulation time increment. This value is then compared with a user specified increment and the lesser is selected as the time increment for use in updating the state of all cryogenic tanks.

Upon the determination of the time increment, the thermodynamic state of the fluid in each tank is updated. The average pressure for the time interval is determined from the initial tank pressure, the initial pressure rise (or decay) rate, and the length of the time interval. The average density for the time increment is determined from the tank volume, the initial weight of cryogen in the tank, and the flowrate. Using these averaged thermodynamic properties, the average pressure change rate is recomputed for each tank. The average pressure change rate and flowrate are then used to update the pressure and density at the end of the time interval. Finally, fluid temperatures are obtained using the thermophysical routines.

In addition to updating the state of each storage tank, the additional flowrates required by the fuel cells to provide power for all electrical equipment operating during the time interval are determined and added to the EPS flow demand. The time required for a complete pressure cycle and heater cycle is also computed for each tank.

One of the basic functions of the model is the determination of the rate of change of tank pressure with respect to time. The method of determining this derivative differs for the two cryogenes since the effects of thermal stratification are considered significant in the oxygen tanks, but not in the hydrogen tanks.

Oxygen Tank. The thermal stratification, resulting from non-uniform heating of the cryogen, significantly affects the operation of the

oxygen tanks. The non-uniform heating leads to higher pressurization rates than that which would result from uniform heating. Furthermore, at high densities, thermally stratified oxygen can experience rapid pressure decay upon mixing due to the thermodynamic properties of the oxygen.

In order to determine the pressure derivative, the oxygen tank is represented by three nodes or volumes. One node (V_1) is associated with the fluid within the tank heater column. A second node (V_2) represents the fluid immediately surrounding the heater column. The final node (V_3) represents the remaining fluid in the tank. The nodal representation of the tank is shown in Figure 9.

The oxygen which flows from the tank is withdrawn from V_3 . Mass interchange is permitted between V_1 and V_2 , but not between V_2 and V_3 . A result of this constraint is that V_2 continuously increases during a mission due to fluid withdrawal from V_3 . The effects of tank stretch and the compression of the fluid in the fill and vent lines (see Appendix II) on the pressure derivative are accounted for in V_3 .

The cylindrical heater is described by a heat source of a specified temperature with a specified heat flux into the two adjacent oxygen nodes. The heater temperature data used in the model were obtained from Apollo 14 flight data and computer simulations of heater operation. The heat flux to the surrounding nodes is calculated from the electrical energy input to the heater, the heater configuration, and the time history of the heater temperature. Heat input is apportioned between the nodes adjacent to the heater by a simple conduction analogy which satisfies a total energy balance for the heater column. Heat conduction is permitted between V_2 and V_3 , but not directly between V_1 and V_2 . The thermal energy exchange between V_1 and V_2 must pass through the heater tube. All external heat leak is applied to V_3 . Heat leak radiant energy transfer is assumed to be negligible.

Mass and energy balance relationships were developed for the fluid in each of the tank nodes. The energy balance equations are:

$$\frac{dp}{dt} = \frac{\phi_1}{V_1} \left\{ q_1 + \dot{m}_1 \left[H(\dot{m}_1)h_2 + H(-\dot{m}_1)h_1 \right] - \dot{m}_1 (h_1 - \theta_1) \right\} \quad (1)$$

$$\frac{dp}{dt} = \frac{\phi_2}{V_2} \left\{ q_2 + \dot{m}_2 \left[H(\dot{m}_2)h_1 + H(-\dot{m}_2)h_2 \right] - \rho_2 \theta_2 \frac{dV_2}{dt} - \dot{m}_2 (h_2 - \theta_2) \right\} \quad (2)$$

and

$$\frac{dp}{dt} = \frac{\phi_3}{V_3} \left\{ q_3 - \rho_3 \theta_3 \frac{dV_3}{dt} + \dot{m}_3 \theta_3 \right\} \quad (3)$$

where:

$$H(x) = \begin{cases} 0 & x < 0 \\ 1 & x \geq 0 \end{cases}$$

$$\frac{dV_3}{dt} = \frac{dV_{\text{tank}}}{dp} \frac{dp}{dt} - \frac{dV_2}{dt} - \frac{dV_L}{dt}$$

The mass balance equations are:

$$\dot{m}_1 = \dot{m}_2$$

$$\dot{m}_3 = \dot{m}_{\text{withdrawal}}$$

The Nomenclature used in these equations is defined in Appendix I.

The mass balance relations may be substituted into Equations (1), (2) and (3) to yield a set of three non-linear equations in the three variables $\frac{dp}{dt}$, \dot{m} , and $\frac{dV_2}{dt}$ which may be solved iteratively. The resulting pressure derivative is then applied as described above.

The pressure collapse potential is defined as the difference between the instantaneous value of pressure and the value that would result from sudden complete mixing of the fluid. Using the individual values of enthalpy for the three volumes, a mean enthalpy is determined for each tank. The mean density of the fluid in each tank is then determined from the known weight of the remaining oxygen and tank volume. The tank pressure for this mixed condition is obtained from the thermophysical routines. Finally, the pressure collapse potential is computed using this pressure and the pressure under stratified conditions.

Hydrogen Tank. During the Apollo 7 Mission, flight tests were performed which demonstrated that thermal stratification did not significantly affect the performance of the hydrogen tanks. It was therefore assumed that thermodynamic equilibrium existed in the hydrogen tanks at all times. The equation which determines the rate of change of pressure with respect to time for the hydrogen tanks is:

$$\frac{dp}{dt} = \frac{\frac{\partial \phi}{\partial V} \dot{m} \left[1 - \frac{3\alpha\rho}{V(1+3\alpha\rho)} \frac{\partial T}{\partial p} \right] + \frac{\phi q}{V}}{\frac{\partial \phi \rho}{1+3\alpha\rho} \frac{\partial T}{\partial \rho} \left[\frac{V_L}{VN_p} + \frac{3r}{2\beta Y} (1-\nu) + 3\alpha \frac{\partial T}{\partial p} \right]} \quad (4)$$

Equation (4) is derived in Appendix II and accounts for variations in tank volume due to fluid pressure and temperature excursions as well as the compression of fluid in the fill and vent lines. All terms of Equation (4) may be determined from the CSS system and fluid thermodynamic properties.

Components and Lines Model

The components and lines model simulates the operation of the Apollo CSS from the tanks to the user subsystems. Given the EPS and ECS flow demands, and the tank conditions, the pressures, temperatures and flowrates are determined at various points in the system. A flow diagram of the model is shown in Figure 10.

The model is divided into two parts which are called, for convenience, the matrix and nodal models. The matrix model is a mathematical representation of the oxygen and hydrogen systems based on the linearized electrical analogs shown in Figures 11 and 12, respectively. A transient, compressible flow analysis of each system is performed to determine the flow rate in each leg and the pressure at each matrix node. The nodal model then uses this information to perform a steady-state, incompressible flow analysis of each leg to determine the pressure at selected locations along that leg and to update the non-linear characteristics of the individual components and line segment resistances. The nodal model also performs a transient thermal analysis of the lines and components. Detailed electrical analogs of the oxygen and hydrogen systems are shown in Figures 13 and 14, respectively.

Matrix Model. The conservation of mass principle is used to determine the matrix node pressures. For any node i , this may be written (see Appendix III)

$$\Sigma I_i = C_i \frac{dE_i}{dt} - I_{R_i} \quad (5)$$

where

$$C_i = \frac{V_i}{2RT_i \sqrt{E_i}} \quad (6)$$

and

$$I_{R_i} = \frac{V_i \sqrt{E_i}}{RT_i^2} \frac{dT_i}{dt} \quad (7)$$

The matrix model solves this set of simultaneous equations for each system by an implicit backward differencing technique. The flow rate in each leg is then evaluated using the conductances in the characteristic matrix.

The program can simulate up to two leaks in each system at any location except downstream of relief valves. Adding a leak is equivalent to adding a matrix node. These are included in the characteristic matrix as floating columns and rows. The flow at leaks is assumed to be choked and is evaluated in the same manner as overboard vents which are discussed below.

Nodal Model. The nodal model performs a steady state analysis of each leg using the matrix model node pressures and temperatures as boundary conditions. The individual components and line segments are analyzed as follows:

Lines and Fittings. The pressure drop in a line segment from inlet i to outlet j is calculated by (see Appendix III):

$$P_i^2 - P_j^2 = \left[\frac{128 L \mu R}{g_c \pi D^4} (T_i + T_j) \right] \dot{m} \quad (8)$$

where

$$T_j = T_k \left[1 - e^{-\left(\frac{UA}{\dot{m}c_p}\right)} \right] + T_i e^{-\left(\frac{UA}{\dot{m}c_p}\right)} \quad (9)$$

Since fluid velocities are small, it is assumed in the derivation of Equation (8) that the flow is laminar and incompressible. The conservation of energy principle is used to determine the line temperatures. It is assumed that conduction through the stand-off brackets and along the lines is negligible. Then, for any node, k ,

$$(mc_p)_k \frac{dT_k}{dt} = \sigma A_k \epsilon_k (T_s^4 - T_k^4) - UA \Delta T_{LM} \quad (10)$$

Fittings have an equivalent L/D of approximately 3. Bends are included by an equivalent L/D which is a function of the bend angle (Figure 15). Clogged lines are simulated by incorporating an increased equivalent length into Equation (8).

Filters, Check Valves, Relief Valves, and Shutoff Valves.

The pressure drops across filters and all open valves are evaluated from Equations (8) and (9). An equivalent L/D of 100 is assumed for filters, open check valves, and open relief valves. The equivalent L/D for open shutoff valves is assumed to be 10. The pressure drop across all closed valves is calculated from:

$$P_i^2 - P_j^2 = \frac{1}{G^m} \quad (11)$$

where the conductance G , is assumed to be 10^{-7} for check valves and 10^{-10} for relief valves. Check valve and relief valve hysteresis is modeled as shown in Figures 16 and 17, respectively. Clogged filters and valves are simulated by incorporating an equivalent L/D that is larger than the nominal value. Failed check valves and relief valves are simulated by incorporating a cracking and/or reseal pressure that will hold the valve open or closed as desired.

The temperature of filters and individual valves are determined from

$$(mc_p)_k \frac{dT}{dt} = - UA \Delta T_{LM}, \quad (12)$$

while the temperatures of valves contained in a valve module housing are determined from

$$(mc_p)_k \frac{dT_k}{dt} = \left(\frac{kA}{\Delta L}\right)_k (T_1 - T_k) - UA \Delta T_{LM} \quad (13)$$

Restrictors. The pressure drop across the oxygen system flow restrictors is evaluated using the data in Figure 18. It is assumed that the process is isothermal.

Overboard Vents. For compressible flow such as overboard venting, the flow is choked. The pressure is evaluated by:

$$P_i = \frac{\sqrt{T_i}}{A_i K_i} \dot{m} \quad (14)$$

The nodal model also checks the solution for convergence. The updated resistance of each component and line segment is compared to the resistance used to calculate the flow rates. If the difference in resistor values is within the convergence criteria, the program proceeds to the next time step; if not, the flow rates are re-evaluated based on the updated resistances. Iteration of the characteristic matrix proceeds in this manner until the solution converges (normally within two iterations).

Auxiliary Routines

In order to adequately simulate the operation of the Cryogenic Storage System, it was necessary to develop several auxiliary routines. Two of the most important routines will be discussed in this section. They are the vehicle thermal model and the thermophysical properties routine.

Vehicle Thermal Model. The vehicle thermal model was developed to compute the Cryogenic Storage System environmental temperatures and to determine the heat leak of the oxygen and hydrogen tanks under normal conditions or under conditions of loss of vacuum in the insulation annulus. The heat leak into the storage tanks is primarily a function of the flowrate through the vapor cooled shroud (VCS) and the temperature in the bay. The bay temperature depends to a large extent upon whether the vehicle is in an inertial hold mode or a passive thermal control mode. The effect of vacuum loss in the jacket is to increase the heat leak into the tank.

Oxygen Tank Heat Leak. The heat leak into the oxygen tanks during nominal operating conditions is computed in the thermal model using empirical data correlations developed by the Beech Aircraft Company (Reference 2). These correlations relate the heat transfer into the oxygen tank with the temperature of the oxygen in storage, the oxygen expulsion rate and the tank outer wall temperature. These correlations are given by the following equations:

$$Q_r = ALI (T_1^{2.5} - T_{vcs}^{2.5}) - \dot{m} (h_{vcs} - h) \quad (15)$$

$$Q_r = AL2 (T_{vcs}^{2.5} - T_2^{2.5}) \quad (16)$$

$$q = AL3 (T_1 - T_2) + .9Q_r \quad (17)$$

The value of the constants which apply to Equations (15), (16), and (17) are as follows:

$$\text{Redesigned Tank: } AL1 = .9205 \times 10^{-5} \text{ BTU/HR}^{\circ R} 2.5$$

$$AL2 = .7278 \times 10^{-5} \text{ BTU/HR}^{\circ R} 2.5$$

$$AL3 = .03775 \text{ BTU/HR}^{\circ R}$$

The amount and temperature of the oxygen in storage is computed in the tankage model of the Integrated Systems Program and is input to the thermal subroutine.

The outer wall tank temperature is computed within the thermal subroutine through a series of data curve fit correlations. The data for these correlations were obtained using the Thermal Mathematical Model (TMM) of the Apollo Service Module. This program is composed of over 800 lumped parameters that constitute a thermal network specifically formatted for solution with the SINDA Multi-Option computer program. Using TMM, a set of parametric computer runs was performed varying the mission mode (inertial hold, passive thermal control or lunar orbit), the quantity of the cryogen in the tanks, and the flowrates from the tanks. A uniform internal tank temperature was assumed in determining the temperature of each oxygen and hydrogen tank surface.

For use in the thermal subroutine, the temperatures computed for the surface of the oxygen tanks by the TMM were averaged for each tank and curve fit as a function of time. The form of the resulting curve fit equations is:

$$T = a_0 + a_1x + a_2x^2 + a_3x^3 \quad (18)$$

where x is the time argument. The coefficients for the polynomial curve fit equations are shown in Table 2. Using these equations, the tank outer wall temperatures are first estimated as a function

of mission mode, time in mode and quantity. These values are then adjusted for the sun look angle. The temperature of the fluid in the VCS is then computed from the temperature of the fluid in storage and the outer wall temperature using an iteration scheme. Once the temperature of the VCS fluid has been determined, the heat flux is computed using Equations (15), (16), and (17).

Hydrogen Tank Heat Leak. The heat leak to the hydrogen tank under nominal operating conditions is computed in the thermal model using data taken from the Apollo Flight Support Handbook (Reference 1). This data, presented in Figure 19, is a correlation of estimated heat flux as a function of the fluid expulsion rate and the quantity of fluid remaining in the tank. This data, however, does not include the effect of temperature in the bay on the heat flux. Since the outer wall temperature is not taken into account, the mission mode cannot be considered in the calculation for the hydrogen tank heat leak. In addition, the discontinuity occurring in the curves at a flow rate of 0.25 lbm/hr does not appear reasonable. Although the correlations presented in Figure 19 do not appear to adequately define the heat leak into the hydrogen tanks, it is the only data currently available. However, if additional data becomes available, the hydrogen tank heat leak correlations used in this portion of the program may be updated easily.

Vacuum Annulus Failure. The nominal pressure in the tank annulus under the design vacuum condition is approximately 2×10^{-9} psia (10^{-7} mm Hg). Depending upon the type of failure, the annulus pressure in the failed condition will be somewhere between the nominal pressure and the annulus burst disc pressure. Burst disc pressures for the oxygen and hydrogen tanks are approximately 75 and 80 psia, respectively. Within these pressure bounds, gas in the annulus may exist in either rarefied or continuum regimes. The criteria for determining the gas regime is based primarily on the ratio of the molecular mean free path to the amount of space available for molecular motion. This ratio is defined as the Knudsen number (K_n). For values of $K_n < 0.01$ the gas is normally treated as continuum flow, while for values of $K_n > 1.0$ the gas is assumed to be in the rarefied regime. For the CSS tanks, an annulus pressure on the order of 10^{-3} psia represents the transition between the two regimes.

The type of analysis used to compute the amount of heat transferred across the annulus depends upon the flow regime. For the rarefied regime the equation for determining the heat flux

per unit area is given by Reference 3 as:

$$\dot{q} = A_c \left(\frac{n+1}{n-1} \right) \frac{\sqrt{R}}{8\pi} \frac{p}{\sqrt{MT}} (T_2 - T_1) \quad (19)$$

For continuum flow regimes, the heat flux per unit area is given by Reference 4 as:

$$\dot{q} = -k \frac{(T_2 - T_1)}{(R_2 - R_1)} \quad (20)$$

An analysis was performed for the Apollo cryogenic storage tanks (Reference 5) assuming residual gas in the annulus consisted of air or the appropriate cryogen. The analysis showed that for an annulus pressure of less than approximately 10^{-7} psia, heat conduction by the residual gas was essentially negligible. However, heat conduction increased rapidly with increasing annulus pressure. The total heat transfer to the tanks as a function of the annulus pressure is shown in graphical form in Figures 20 and 21. These curves have been incorporated into the thermal model such that when the thermal subroutine encounters a failed tank flag, the data presented in the figures is used to determine the heat flux to the tank based upon the vacuum jacket pressure. This pressure is an input to the program.

Components and Line Environmental Temperatures. The environmental temperatures used to determine the state of the fluid in the components and lines were obtained in a manner identical to the tank environmental temperatures. The Thermal Mathematical Model of the Apollo Service Module was used to obtain data at several locations as given in Table 3. These data were incorporated into the Integrated Systems Program as a series of curve fit correlations. The form of the resulting equation is the same as Equation (18). The coefficients for the curve fit equations are presented in Table 2.

The TMM did not model the Command Module (CM) cabin, the CM Reaction Control System Tank Annulus, or the ECS umbilical. The temperature at these locations was assumed to be 70°F.

Thermophysical Properties for Oxygen and Hydrogen. Computer subroutines for computing the thermophysical properties for oxygen and hydrogen were developed and included into the Integrated Systems Program. The majority of the data used in these subroutines was

recommended by the National Bureau of Standards (NBS). That data not available from the NBS was taken from Reference 6 (Stewart). In general these subroutines determine pressure (p), temperature (T), density (ρ), enthalpy (h), the specific heat at constant pressure (c_p), the specific heat at constant volume (c_v), viscosity (μ), thermal conductivity (k), isotherm and isochor derivatives and the functions ϕ and Θ , providing sufficient information concerning the fluid state is known. The data is included in the subroutines both in equation and table form. A routine is also included in the subroutines for interpolating between values from the tables.

Oxygen Properties. Data contained in the subroutines for computing the thermophysical properties of oxygen were taken from References 6, 7, and 8. Reference 6 presents an equation of state for oxygen determined by R. B. Stewart. The isotherm and isochor derivatives were derived from this equation. While Reference 7 (Weber) also presents data for the isotherm and isochor derivatives, the results derived from Reference 6 are valid for a greater range. Both sets of data were included in the thermophysical subroutines to provide greater flexibility since the derivatives derived from Reference 6 may be determined with known values of temperature and density, while the data from Reference 7 uses either pressure and temperature or pressure and density.

The equation of state provided by Reference 6 may be used to compute pressure from known values of density and temperature. This equation is valid for temperatures between 117 and 540°R and for pressures to 5000 psia. The equation of state is as follows:

$$\begin{aligned}
 p = & \rho R T + (n_1 T + n_2 + n_3/T^2 + n_4/T^4 + n_5/T^6) \rho^2 \\
 & + (n_6 T^2 + n_7 T + n_8 + n_9/T + n_{10}/T^2) \rho^3 \\
 & + (n_{11} T + n_{12}) \rho^4 + (n_{13} + n_{14} T) \rho^5 \\
 & + \rho^3 (n_{15}/T^2 + n_{16}/T^3 + n_{17}/T^4) \exp(n_{25} \rho^2) \\
 & + \rho^5 (n_{18}/T^2 + n_{19}/T^3 + n_{20}/T^4) \exp(n_{25} \rho^2) \\
 & + \rho^7 (n_{21}/T^2 + n_{22}/T^3 + n_{23}/T^4) \exp(n_{25} \rho^2) \\
 & + n_{24} \rho^{(n_{28}+1)} (\rho^{n_{28}-\rho} c^{n_{28}}) \exp \left[n_{26} (\rho^{n_{28}-\rho} c^{n_{28}})^2 + n_{27} (T-T_c)^2 \right] \quad (21)
 \end{aligned}$$

where: $\rho_c = 13.333$ gmol/liter, critical density

$T_c = 154.77$ °K, critical temperature

In this expression, p is in atmospheres, T is in °K, and ρ is in gmol/liter. The constants for this equation are given in Table 4. The subroutine in which Equation (21) is programmed converts the units of density from lbm/cu-ft to gmol/liter and temperature from °R to °K prior to use. The output pressure is in psia.

The isotherm derivative, $\left. \frac{\partial p}{\partial \rho} \right|_T$, is the partial derivative of Equation (21) with respect to the density at constant temperature and is given by:

$$\left. \frac{\partial p}{\partial \rho} \right|_T = R T + \sum_{i=1}^{24} n_i X_i \quad (22)$$

Values for the variables in this equation are presented in Table 5.

The coefficients n_i are the same as those for Equation (21). The subroutine which computes the isotherm derivative converts density from lbm/cu-ft to gmol/liter and temperature from °R to °K prior to its use in Equation (22). The output derivative is in units of psia-ft³/lbm.

The isochor derivative $\left. \frac{\partial p}{\partial T} \right|_{\rho}$, is the partial derivative of Equation (21) with respect to temperature at constant density and is given by:

$$\left. \frac{\partial p}{\partial T} \right|_{\rho} = \rho R + \sum_{i=1}^{24} n_i X_i \quad (23)$$

where the coefficients n_i are the same as those listed for Equation (21). The variables in this equation are shown in Table 6. The conversion from one set of units to the other is performed the same as for Equations (21) and (22). The output derivative is in units of psia/°R.

In addition to providing data for the isotherm derivative and the isochor derivative, Reference 7 presents data for density, enthalpy, specific heats (at constant pressure and volume) and the functions θ and ϕ . All are in tabular form. Further flexibility was provided by permitting these properties to be determined from known values of pressure and temperature or from pressure and density. These tables are valid for temperatures from 100 to 540°R at 5 degree increments and for pressures ranging from 367 to 1250 psia at increments of 73.5 psi. Table 7 lists the thermophysical parameters which are available.

Data from Reference 8 is also in the form of tables and provides viscosity and thermal conductivity as functions of pressure and temperature. This data is valid for temperatures ranging from 180 to 540°R at increments of 18 degrees and for pressures from 367 to 1250 psia at increments of 73.5 psi.

Hydrogen Properties. The thermophysical properties used in the hydrogen subroutine are based upon computer programs developed by the NBS (Reference 9). These properties are valid for pressures from 1 to 5000 psia and for temperatures ranging from 25 to 5000 °R. In the NBS programs all thermophysical properties are determined from known values of pressure and temperature and include enthalpy, density, specific heats for both constant pressure and constant volume, viscosity and thermal conductivity. However, in the subroutine developed for the Integrated System Program, provision was made to compute the pressure and temperature from other known properties as described below. The pressure, density and temperature are in units of psia, lbm/ft³, and °R, respectively.

The NBS program expresses hydrogen density as a polynomial equation in terms of pressure and temperature, $\rho = \rho(p,T)$. The equation has been programmed such that pressure may be determined from this equation as a function of density and temperature using a Newton-Raphson iteration method. An a priori value of pressure is required to initiate the iteration and should be estimated as closely as possible to the actual value. Temperature is computed in a manner similar to that of pressure from this same expression.

The available parameters are listed in Table 7.

REFERENCES

1. NASA Document, "Apollo Fuel Cell and Cryogenic Gas Storage System Flight Support Handbook," Manned Spacecraft Center, Houston, Texas, 18 February 1970.
2. Analysis of Oxygen Tank Heat Leak, obtained informally from Beech Aircraft Co., Boulder, Colorado.
3. Corruccini, R. J., "Gaseous Heat Conduction at Low Pressures and Temperatures," Vacuum, Vol. VII and VIII, April, 1959.
4. McAdams, W. H., "Heat Transmission," McGraw-Hill Cook Company, 3rd Edition, 1954.
5. TRW IOC 70.4354.3-104, "Effect of CSS Tank Vacuum Annulus Leakage on Heat Transfer Rates," P. J. Knowles, 23 November 1970.
6. Stewart, R. B., "The Thermodynamic Properties of Oxygen," PhD Thesis, University of Iowa, June, 1966.
7. Weber, L. A., "Thermodynamic and Related Properties of Oxygen from the Triple Point to 300°K at Pressures to 330 Atmospheres," NBS Report 9710A, 29 August 1968.
8. Roder, H. M., "Viscosity and Thermal Conductivity of Oxygen," NBS letter 275.02 to J. Smithson, EP5, NASA/MSC, September 24, 1970.
9. Hall, W. J., R. D. McCarty, and H. M. Roder, "Computer Programs for Thermodynamic and Transport Properties of Hydrogen," NBS Report #9288, (NASA-CR88086), August, 1967.

TABLE 1

CRYOGENIC SYSTEM OPERATIONAL PARAMETERS

| | <u>Hydrogen</u> | <u>Oxygen</u> |
|-------------------------------------|--------------------------|----------------------------|
| TANK MATERIAL | 5 Al-2.5 Sn ELI t1 | Inconel 718 |
| TANK WEIGHT (PER TANK) | | |
| Empty (Approx) | 80.00 lb. | 90.82 lb. |
| Usable Fluid | 28.15 lb. | 323.45 lb. |
| Stored Fluid (100% indication) | 29.31 lb. | 330.1 lb. |
| Residual | 4% | 2% |
| Maximum Fill Quantity | 30.03 lb. | 337.9 lb. |
| TANK VOLUME (PER TANK) | 6.80 ft ³ | 4.75 ft ³ |
| TANK PRESSURIZATION | | |
| Heaters elements per tank | 2 | 3 |
| Flight Resistance | 78.4 ohms per element | 18.45 ohms per element |
| Nominal Voltage | 28 V DC | 28 V DC |
| Power | 10 watts per element* | 42.5 watts per element* |
| Total Heater Heat Input Per tank | 68.2 BTU/Hr | 434.8 BTU/Hr |
| Ground Resistance | 78.4 ohms per element | 18.45 ohms per element |
| Voltage | 28 V DC | 28 V DC |
| Power | 10 watts per element* | 42.5 watts per element* |
| Total Heater Heat Input Per Tank | 68.2 BTU/Hr | 434.8 BTU/Hr |

TABLE 1 (Continued)

| | <u>Hydrogen</u> | <u>Oxygen</u> |
|--|--|---------------|
| Pressure Switch | | |
| Open Pressure Max. | 260 psia | 935 psia |
| Close Pressure Min. | 225 psia | 865 psia |
| Deadband Min. | 10 psia | 30 psia |
| Destratification Motors (2 Motors Per Tank) | | |
| Voltage | 115/200 V 400 cps | None |
| Power - Average | 3.5 watts per motor* | None |
| Total Average Motor | 23.8 BTU/Hr | None |
| Heat Input Per Tank | | |
| SYSTEM PRESSURES | | |
| Normal Operating | 245 ± 15 psia | 900 ± 35 psia |
| Spec Min. Dead Band of Pressure Switches | 10 psi | 30 psi |
| Relief Valve Note: | Relief Valves are referenced to environmental pressure, therefore pressure at sea level (psig) will be the same value in vacuum (psia) | |
| Crack Min. | 273 psig | 938 psig |
| Full Flow Max. | 285 psig | 1010 psig |
| Reseat Min. | 268 psig | 865 psig |
| Outer Tank Shell Burst Disc | | |
| Nominal Burst Pressure | 90 ± 10 -20 psid | 75 ± 7.5 psid |
| SYSTEM TEMPERATURES | | |
| Stored Fluid | -425 to 80°F | -300 to 80°F |
| *Conversion Factor: 1 watt = 3.41 BTU/Hr | | |

TABLE 2

CURVE FIT COEFFICIENTS REPRESENTATIVE
OF THE CSS THERMAL ENVIRONMENT

| Mission Mode | Node | a_0 (°F) | a_1 (°F/Hr) | a_2 (°F/Hr ²) | a_3 (°F/Hr ³) | T_{inf} °F | Time Argument | |
|--------------|-------------|---------------|------------------|--------------------------------|--------------------------------|-----------------|---------------|--|
| | | | | | | | t+3 (Hrs) | $\frac{1}{t+3}$ (Hrs) ⁻¹ |
| PTC | Tanks 1 & 2 | 46.152 | 35.715 | 105.97 | -38.106 | | | X |
| PTC | Tank 3 | 25.164 | 73.761 | 202.92 | -112.08 | | | X |
| Hot Soak | Tanks 1 & 3 | 60.0 | 4.44 | .0 | 0.0 | | X | |
| Hot Soak | Tank 2 | 58.523 | 31.715 | -3.57 | 0.1277 | | X | |
| Cold Soak | Tanks 1 & 3 | -15.824 | 368.40 | -485.5 | 232.26 | | | X |
| Cold Soak | Tank 2 | -61.812 | 549.39 | -650.84 | 283.34 | | | X |
| PTC | 150 | 66.0 | 0.0 | 0.0 | 0.0 | 66.0 | | X |
| PTC | 151 | 85.3 | -64.0 | 0.0 | 0.0 | 80.0 | | X |
| PTC | 152 | 47.0 | 0.0 | 0.0 | 0.0 | 47.0 | | X |
| PTC | 153 | 49.5 | 28.6 | 0.0 | 0.0 | 57.0 | | X |
| PTC | 154 | 42.5 | 46.5 | 0.0 | 0.0 | 48.0 | | X |
| PTC | 155 | 117.3 | -130.0 | 0.0 | 0.0 | 101.0 | | X |
| PTC | 156 | 132.4 | -145.3 | 0.0 | 0.0 | 118.0 | | X |
| PTC | 157 | 91.8 | -77.3 | 0.0 | 0.0 | 86.0 | | X |
| PTC | 158 | 70.0 | 0.0 | 0.0 | 0.0 | 70.0 | | X |
| PTC | 159 | 48.4 | 18.2 | 0.0 | 0.0 | 49.0 | | X |
| PTC | 163 | 47.0 | 0.0 | 0.0 | 0.0 | 47.0 | | X |
| Cold Soak | 150 | 80.0 | -3.9 | 0.27 | 0.0 | 56.0 | | X |

359

TABLE 2 (Cont'd)

CURVE FIT COEFFICIENTS REPRESENTATIVE
OF THE CSS THERMAL ENVIRONMENT

| Mission Mode | Node | a_0 (°F) | a_1 (°F/Hr) | a_2 (°F/Hr ²) | a_3 (°F/Hr ³) | T_{inf} °F | Time Argument | |
|--------------|------|---------------|------------------|--------------------------------|--------------------------------|-----------------|---------------|--|
| | | | | | | | t+3 (Hrs) | $\frac{1}{t+3}$ (Hrs) ⁻¹ |
| Cold Soak | 151 | 115.2 | -18.6 | 1.4 | -0.036 | 31.0 | | X |
| Cold Soak | 152 | 109.3 | -22.3 | 1.7 | -0.041 | 5.0 | | X |
| Cold Soak | 153 | 88.7 | -10.2 | 0.45 | -0.0074 | 7.0 | | X |
| Cold Soak | 154 | 107.5 | -18.3 | 1.2 | -0.03 | 6.0 | | X |
| Cold Soak | 155 | 60.7 | -0.25 | 0.046 | -0.0021 | 58.0 | | X |
| Cold Soak | 156 | 51.3 | 7.65 | -0.42 | 0.0067 | 96.0 | | X |
| Cold Soak | 157 | 99.6 | -12.6 | 1.07 | -0.029 | 50.0 | | X |
| Cold Soak | 158 | 50.0 | 5.8 | -0.26 | 0.0039 | 96.0 | | X |
| Cold Soak | 159 | 111.6 | -20.1 | 1.42 | -0.035 | 5.0 | | X |
| Cold Soak | 163 | 32.1 | 12.2 | -0.70 | -0.013 | 109.0 | | X |
| Hot Soak | 150 | 103.3 | -10.2 | 0.812 | -0.002 | 50.0 | | X |
| Hot Soak | 151 | 47.7 | 8.73 | -0.443 | 0.00071 | 103.0 | | X |
| Hot Soak | 152 | 32.1 | 12.2 | -0.7 | 0.013 | 109.0 | | X |
| Hot Soak | 153 | 105.2 | 75.8 | -882.4 | 396.6 | 105.0 | | X |
| Hot Soak | 154 | 97.2 | 62.1 | -870.3 | 395.0 | 99.0 | | X |
| Hot Soak | 155 | 120.7 | 40.4 | -975.4 | 450.0 | 122.0 | | X |
| Hot Soak | 156 | 24.6 | 17.9 | -0.892 | 0.013 | 136.0 | | X |
| Hot Soak | 157 | 17.0 | 17.6 | -1.2 | 0.028 | 105.0 | | X |

TABLE 2 (Cont'd)

CURVE FIT COEFFICIENTS REPRESENTATIVE
OF THE CSS THERMAL ENVIRONMENT

| Mission Mode | Node | a ₀ (°F) | a ₁ (°F/Hr) | a ₂ (°F/Hr ²) | a ₃ (°F/Hr ³) | T _{inf} °F | Time Argument | |
|--------------|------|------------------------|---------------------------|---|---|------------------------|---------------|--|
| | | | | | | | t+3 (Hrs) | $\frac{1}{t+3}$ (Hrs) ⁻¹ |
| Hot Soak | 158 | 86.1 | -6.2 | 0.2 | -0.0021 | 25.0 | | X |
| Hot Soak | 159 | 102.2 | 63.1 | -885.9 | 401.9 | 10.0 | | X |
| Hot Soak | 163 | 109.3 | -22.3 | 1.7 | -0.041 | 5.0 | | X |
| Lunar Orbit | 150 | 53.5 | 5.5 | 0.0 | 0.0 | 114.0 | X | |
| Lunar Orbit | 151 | 74.6 | -1.52 | 0.0 | 0.0 | 54.0 | X | |
| Lunar Orbit | 152 | 45.0 | 0.0 | 0.0 | 0.0 | 45.0 | X | |
| Lunar Orbit | 153 | 79.0 | 0.0 | 0.0 | 0.0 | 79.0 | X | |
| Lunar Orbit | 154 | 58.0 | 0.0 | 0.0 | 0.0 | 58.0 | X | |
| Lunar Orbit | 155 | 51.1 | 2.63 | 0.0 | 0.0 | 84.0 | X | |
| Lunar Orbit | 156 | 58.9 | 3.89 | 0.0 | 0.0 | 107.0 | X | |
| Lunar Orbit | 157 | 69.0 | 0.0 | 0.0 | 0.0 | 69.0 | X | |
| Lunar Orbit | 158 | 76.72 | -2.24 | 0.0 | 0.0 | 42.0 | X | |
| Lunar Orbit | 159 | 57.0 | 0.0 | 0.0 | 0.0 | 57.0 | X | |
| Lunar Orbit | 163 | 45.0 | 0.0 | 0.0 | 0.0 | 45.0 | X | |

$$T = a_0 + a_1X + a_2X^2 + a_3X^3 \text{ where } X = \text{time argument}$$

TABLE 3

ENVIRONMENTAL TEMPERATURE LOCATIONS

| SINK INDEX | LOCATION |
|------------|---------------------|
| 150 | TUNNEL |
| 151 | Bay 4 |
| 152 | Bay 4 |
| 153 | Forward Bulkhead |
| 154 | Bay 4 |
| 155 | Bay 4 |
| 156 | Bay 4 |
| 157 | Bay 4 |
| 158 | Forward Bulkhead |
| 159 | Forward Bulkhead |
| 160 | Umbilical |
| 161 | CM RCS Tank Annulus |
| 162 | CM Cabin |
| 163 | Bay 1 |

TABLE 4

CONSTANTS FOR STEWART'S EQUATION OF STATE

| | |
|--------------------------------------|--------------------------------------|
| $R = 0.0820535$ | $n_{15} = 1.73655508 \times 10^2$ |
| $n_1 = 3.38759078 \times 10^{-3}$ | $n_{16} = 3.01752841 \times 10^5$ |
| $n_2 = -1.31606223$ | $n_{17} = -3.49528517 \times 10^7$ |
| $n_3 = 1.92049067 \times 10^3$ | $n_{18} = 8.86724004 \times 10^{-1}$ |
| $n_4 = 1.92049067 \times 10^7$ | $n_{19} = -2.67817667 \times 10^2$ |
| $n_5 = -2.90260005 \times 10^{10}$ | $n_{20} = 1.05670904 \times 10^5$ |
| $n_6 = -5.70101162 \times 10^{-8}$ | $n_{21} = 5.63771075 \times 10^{-3}$ |
| $n_7 = 7.96822375 \times 10^{-5}$ | $n_{22} = -1.12012813$ |
| $n_8 = 6.07022502 \times 10^{-3}$ | $n_{23} = 1.46829491 \times 10^2$ |
| $n_9 = -2.71019658$ | $n_{24} = 9.98868924 \times 10^{-4}$ |
| $n_{10} = -3.59419602 \times 10$ | $n_{25} = -0.00560$ |
| $n_{11} = 1.02209557 \times 10^{-6}$ | $n_{26} = -0.157$ |
| $n_{12} = 1.90454505 \times 10^{-4}$ | $n_{27} = -0.350$ |
| $n_{13} = 1.21708394 \times 10^{-5}$ | $n_{28} = 0.90$ |
| $n_{14} = 2.44255945 \times 10^{-3}$ | |

TABLE 5 - VARIABLES FOR COMPUTING ISOTHERM DERIVATIVES

$$\begin{array}{ll}
 X_1 = 2\rho T & X_{13} = 5\rho^4 \\
 X_2 = 2\rho & X_{14} = 5\rho^4/T \\
 X_3 = 2\rho/T^2 & X_{15} = f_6/T^2 \\
 X_4 = 2\rho/T^4 & X_{16} = f_6/T^3 \\
 X_5 = 2\rho/T^6 & X_{17} = f_6/T^4 \\
 X_6 = 3\rho^2 T^2 & X_{18} = f_7/T^2 \\
 X_7 = 3\rho^2 T & X_{19} = f_7/T^3 \\
 X_8 = 3\rho^2 & X_{20} = f_7/T^4 \\
 X_9 = 3\rho^2/T & X_{21} = f_8/T^2 \\
 X_{10} = 3\rho^2/T^2 & X_{22} = f_8/T^3 \\
 X_{11} = 4\rho^3 T & X_{23} = f_8/T^4 \\
 X_{12} = 4\rho^3 & \\
 X_{24} = f_9 f_2 f_3 + \rho^{(n_{28}+1)} f_{10} f_3 + \rho^{(n_{28}+1)} f_2 f_{11} &
 \end{array}$$

$$\begin{array}{ll}
 f_1 = \exp(n_{25} \rho^2) & f_6 = 3f_1 \rho^2 + f_5 \rho^3 \\
 f_2 = \rho^{n_{28}} - \rho^{n_{28}} c_2 & f_7 = 5f_1 \rho^4 + f_5 \rho^5 \\
 f_3 = \exp[n_{26} f_2 + n_{27} (T - T_c)^2] & f_8 = 7f_1 \rho^6 + f_5 \rho^7 \\
 f_4 = 2n_{27} (T - T_c) f_3 & f_9 = (n_{28} + 1) \rho^{n_{28}} \\
 f_5 = 2f_1 \rho^{n_{25}} & f_{10} = n_{28} \rho^{(n_{28}-1)} \\
 & f_{11} = 2f_2 n_{26} f_3 f_{10}
 \end{array}$$

TABLE 6

VARIABLES FOR COMPUTING ISOCHOR DERIVATIVE

| | |
|-------------------------|--------------------------------------|
| $X_1 = \rho^2$ | $X_{13} = 0$ |
| $X_2 = 0$ | $X_{14} = -\rho^5/T^2$ |
| $X_3 = -2\rho^2/T^3$ | $X_{15} = -2\rho^3 f_1/T^3$ |
| $X_4 = -4\rho^2/T^5$ | $X_{16} = -3\rho^3 f_1/T^4$ |
| $X_5 = -6\rho^2/T^7$ | $X_{17} = -4\rho f_1/T^5$ |
| $X_6 = 2T\rho^3$ | $X_{18} = -2\rho^5 f_1/T^3$ |
| $X_7 = \rho^3$ | $X_{19} = -3\rho^5$ |
| $X_8 = 0$ | $X_{20} = -4\rho^5 f_1/T^5$ |
| $X_9 = -\rho^3/T^2$ | $X_{21} = -2\rho^7 f_1/T^3$ |
| $X_{10} = -2\rho^3/T^3$ | $X_{22} = -3\rho^7 f_1/T^4$ |
| $X_{11} = \rho^4$ | $X_{23} = -4\rho^7 f_1/T^5$ |
| $X_{12} = 0$ | $X_{24} = \rho^{(n_{28}+1)} f_2 f_4$ |

where: $f_1 = \exp(n_{28}\rho^2)$

$$f_2 = \rho^{n_{28}} - \rho_c^{n_{28}}$$

TABLE 7

THERMOPHYSICAL PROPERTIES SUBROUTINES

| PROPERTY | UNITS | INPUT VARIABLES | REFERENCE |
|----------------------------------|---------------------------|-----------------|-----------|
| OXYGEN | | | |
| Density | lbm/ft ³ | P&T | 7 |
| Enthalpy | btu/lbm | P&T | 7 |
| Enthalpy | btu/lbm | P& ρ | 7 |
| Function Θ | btu/lbm | P&T | 7 |
| Function ϕ | psia-ft ³ /btu | P&T | 7 |
| Isochor | psia/°R | T& ρ | 6 |
| Isochor | psia/°R | P&T | 7 |
| Isochor | psia/°R | P& ρ | 7 |
| Isotherm | psia-ft ³ /btu | T& ρ | 6 |
| Isotherm | psia-ft ³ /btu | P&T | 7 |
| Isotherm | psia-ft ³ /btu | P& ρ | 7 |
| Pressure | Psia | T& ρ | 6 |
| Specific Heat, C _P | btu/lbm-°R | P&T | 7 |
| Specific Heat, C _P | btu/lbm-°R | P& ρ | 7 |
| Specific Heat, C _V | btu/lbm-°R | P&T | 7 |

TABLE 7 (CONT'D)
THERMOPHYSICAL PROPERTIES SUBROUTINES

| PROPERTY | UNITS | INPUT VARIABLES | REFERENCE |
|---------------------------|------------------------------------|-----------------|-----------|
| OXYGEN | | | |
| Specific Heat, C_v | btu/lbm-°R | P&ρ | 7 |
| Thermal Conduc- tivity | btu(ft/hr)/ ft ² /°R | P&T | 8 |
| Temperature | °R | P&ρ | 7 |
| Viscosity | lbf-hr/ft ² | P&T | 8 |
| HYDROGEN | | | |
| Density | lbm/ft ³ | P&T | 9 |
| Enthalpy | btu/lbm | P&T | 9 |
| Function θ | btu/lbm | P&T | 9 |
| Function φ | psia-ft ³ /btu | P&T | 9 |
| Isochor | psia/°R | P&T | 9 |
| Isotherm | psia-ft ³ /btu | P&T | 9 |
| Pressure | Psia | T&ρ | 9 |
| Specific Heat, C_p | btu/lbm-°R | P&T | 9 |
| Specific Heat, C_v | btu/lbm-°R | P&T | 9 |
| Thermal Conduc- tivity | btu(ft/hr)/ ft ² /°R | P&T | 9 |
| Temperature | °R | P&ρ | 9 |
| Viscosity | lbf-hr/ft ² | P&T | 9 |

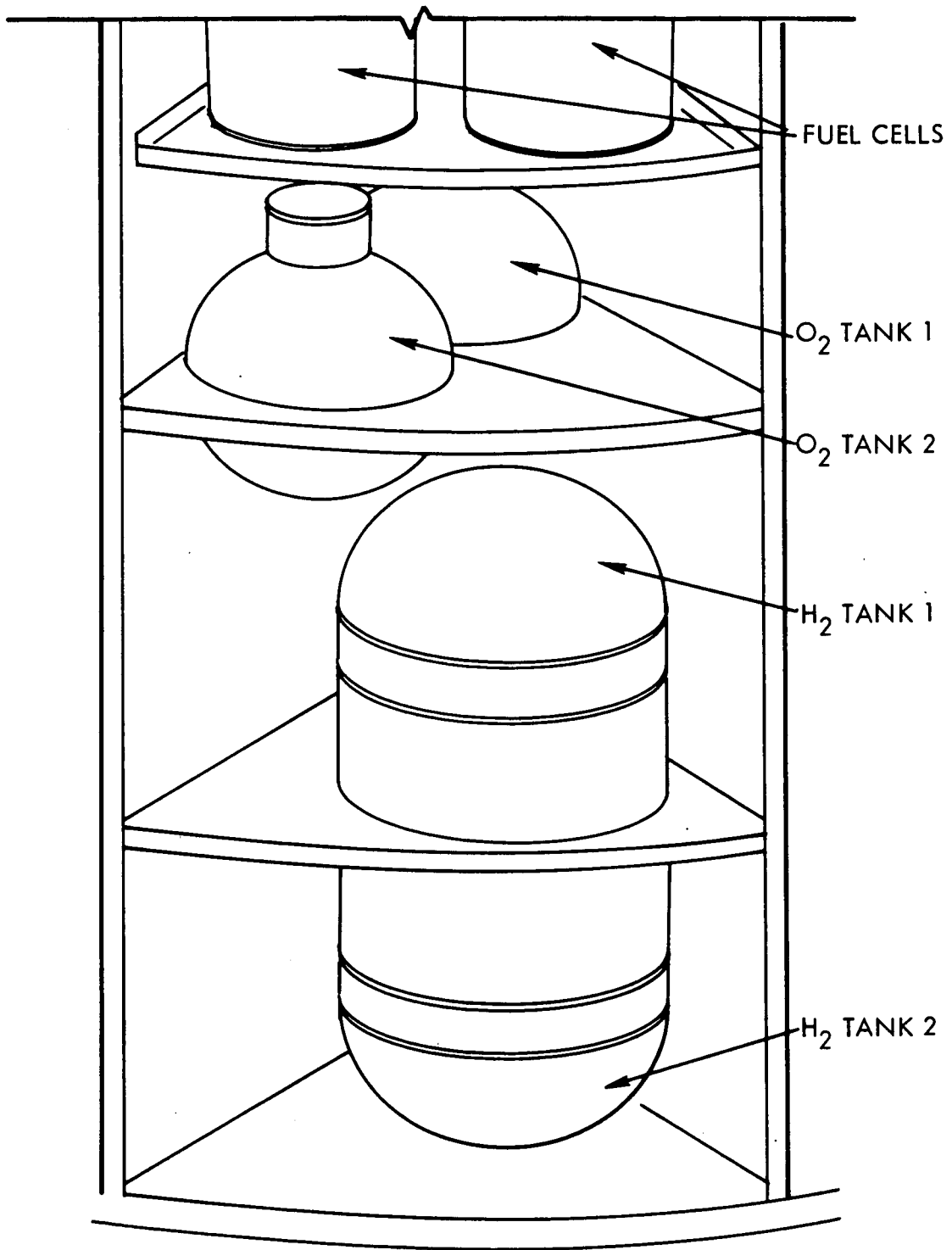


FIGURE 1. SM SECTOR IV CSS TANKAGE ARRANGEMENT

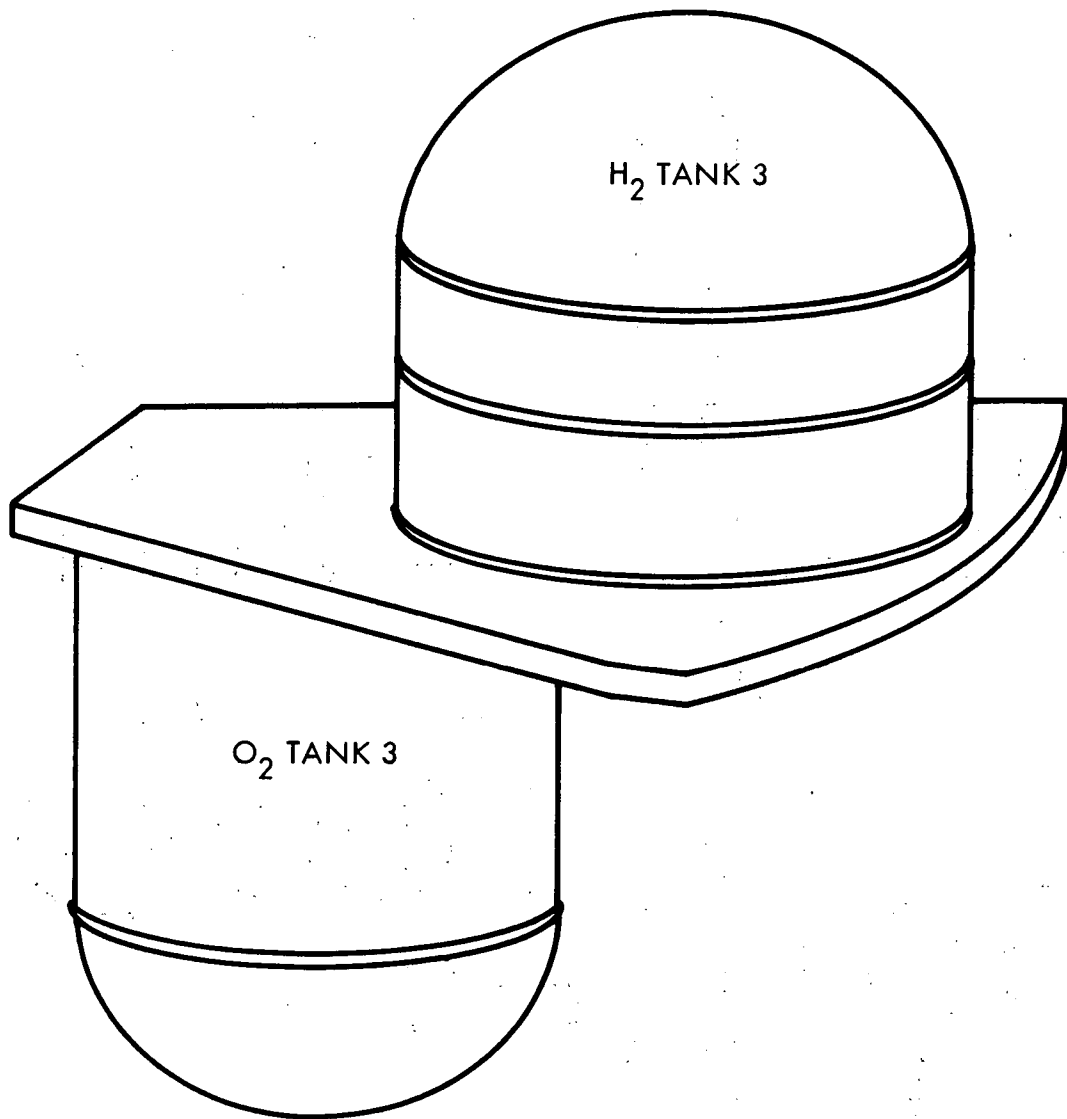
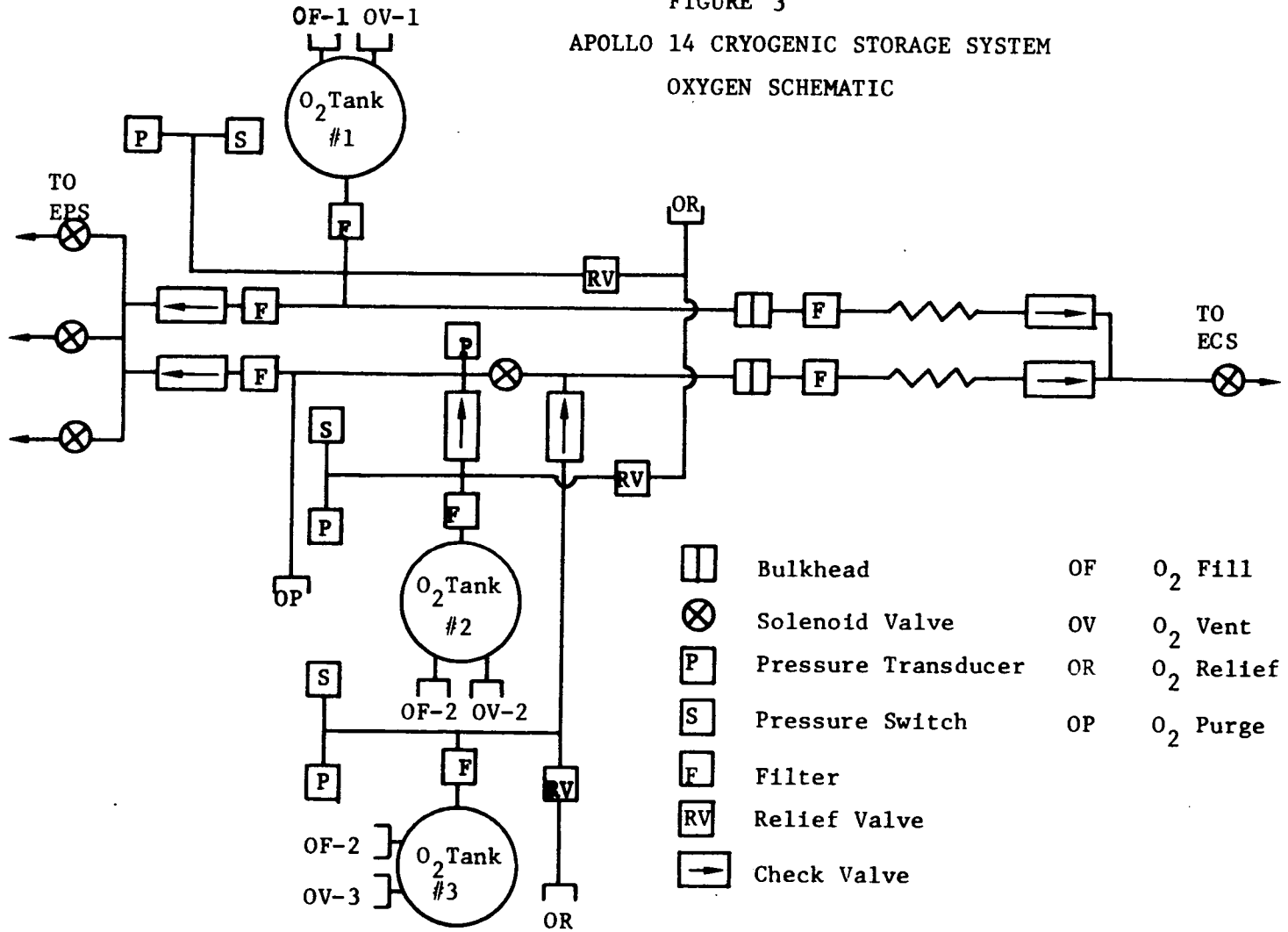


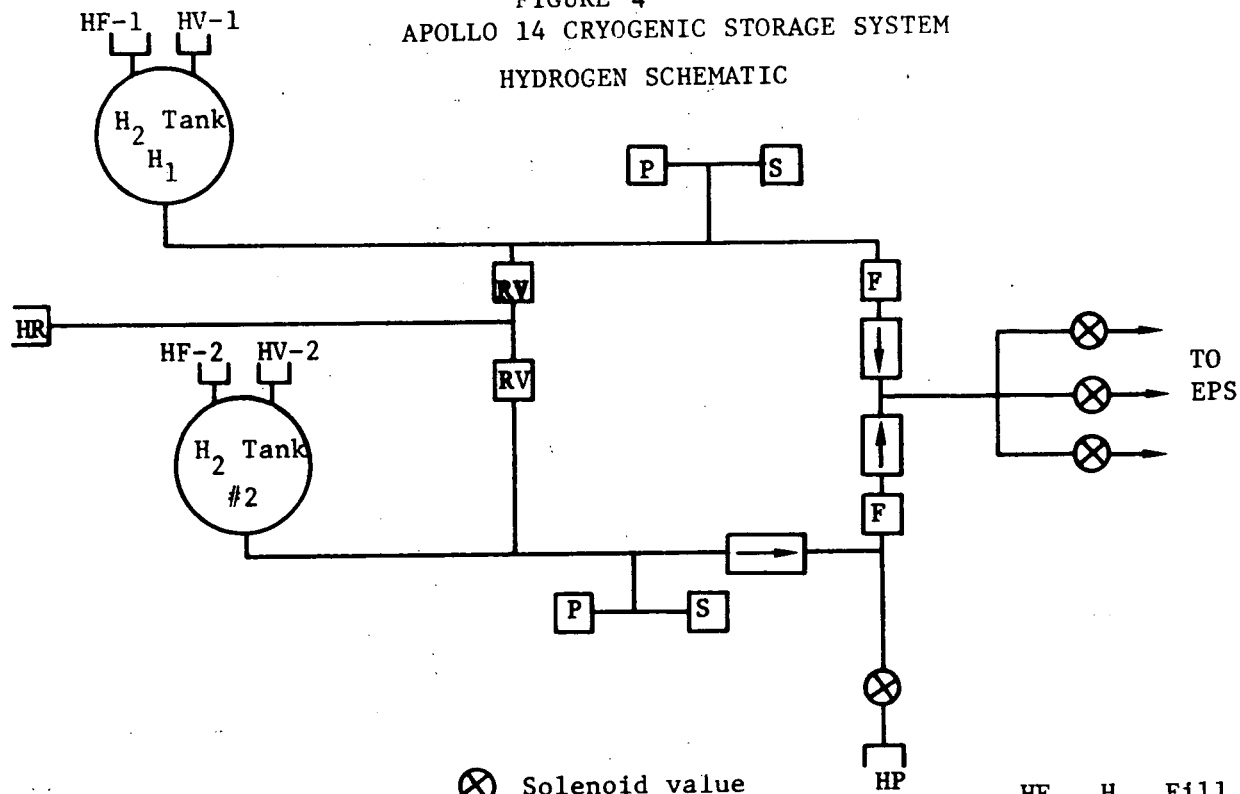
FIGURE 2. SM SECTOR I CSS TANKAGE ARRANGEMENT

FIGURE 3
 APOLLO 14 CRYOGENIC STORAGE SYSTEM
 OXYGEN SCHEMATIC



370

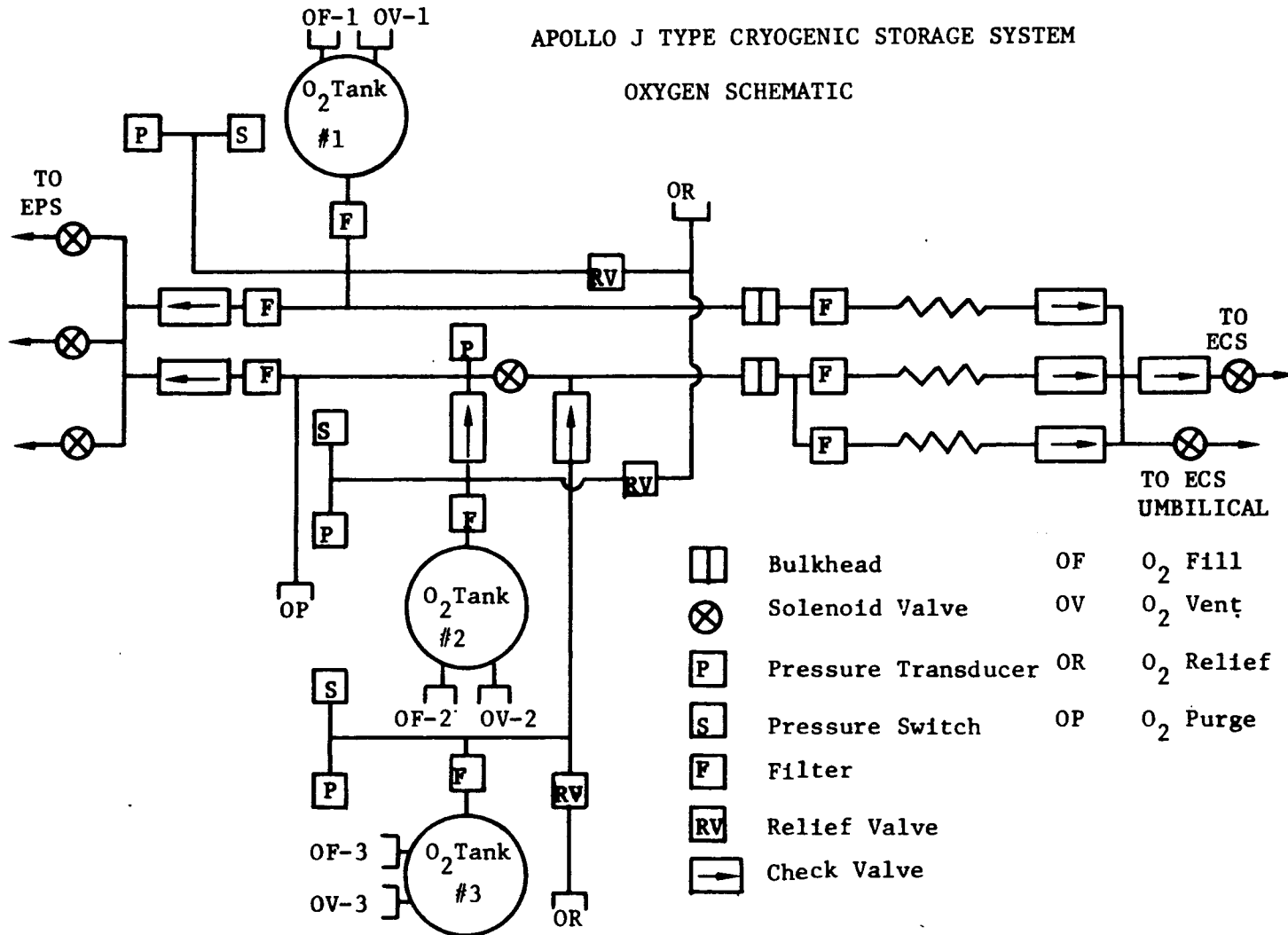
FIGURE 4
 APOLLO 14 CRYOGENIC STORAGE SYSTEM
 HYDROGEN SCHEMATIC










371

- | | | | | |
|----|--------------------|----|----------------|------------|
| ⊗ | Solenoid valve | HF | H ₂ | Fill |
| P | Pressure Transduce | HV | H ₂ | Vent |
| S | Pressure Switch | HR | H ₂ | Relief |
| F | Filter | HP | H ₂ | Purge Port |
| RV | Relief Valve | | | |
| → | Check Valve | | | |

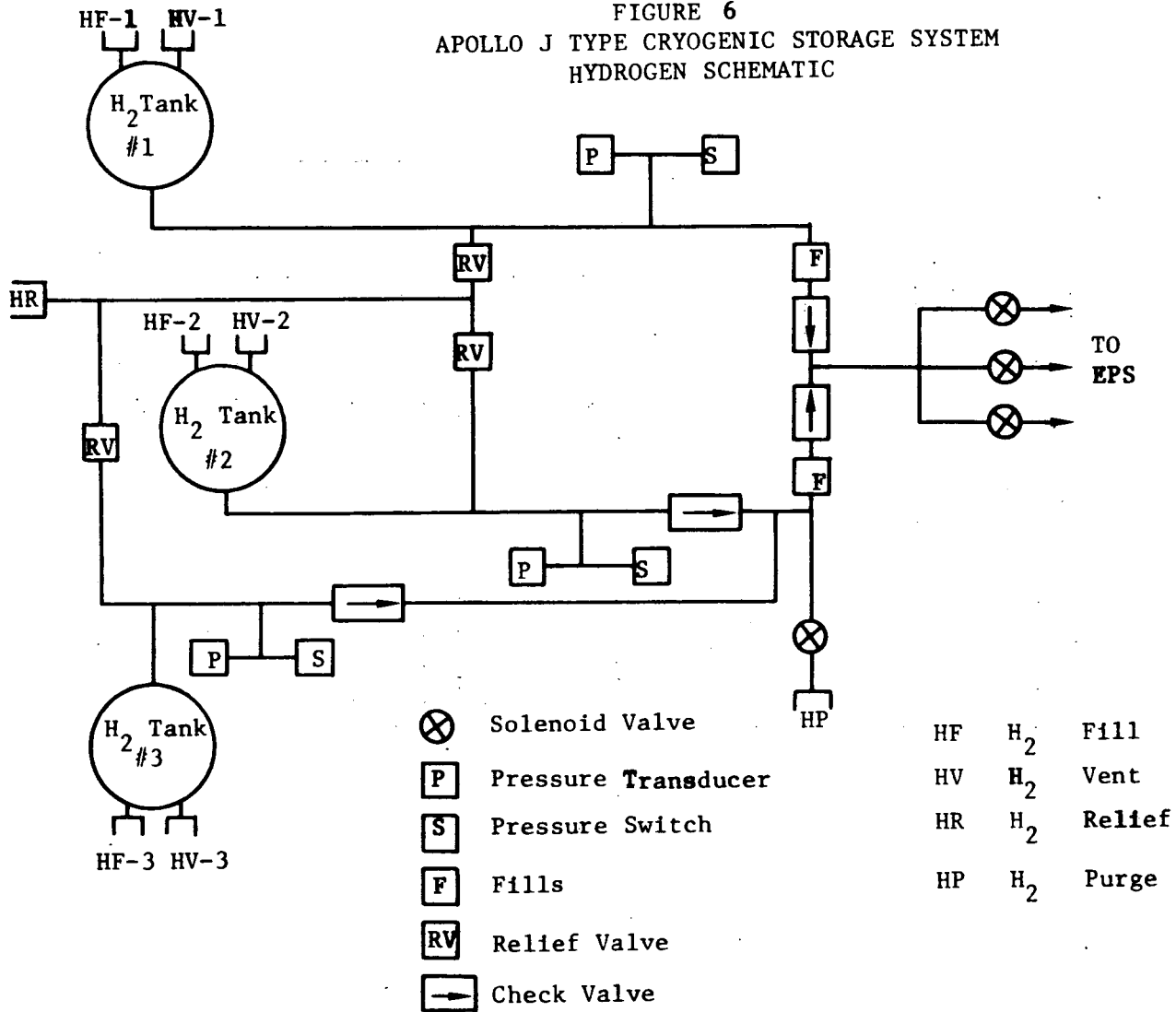
FIGURE 5.
 APOLLO J TYPE CRYOGENIC STORAGE SYSTEM
 OXYGEN SCHEMATIC



- | | | | |
|---|---------------------|----|-----------------------|
|  | Bulkhead | OF | O ₂ Fill |
|  | Solenoid Valve | OV | O ₂ Vent |
|  | Pressure Transducer | OR | O ₂ Relief |
|  | Pressure Switch | OP | O ₂ Purge |
|  | Filter | | |
|  | Relief Valve | | |
|  | Check Valve | | |

372

FIGURE 6
 APOLLO J TYPE CRYOGENIC STORAGE SYSTEM
 HYDROGEN SCHEMATIC



373

FIGURE 7
INTEGRATED SYSTEMS PROGRAM
FLOW DIAGRAM

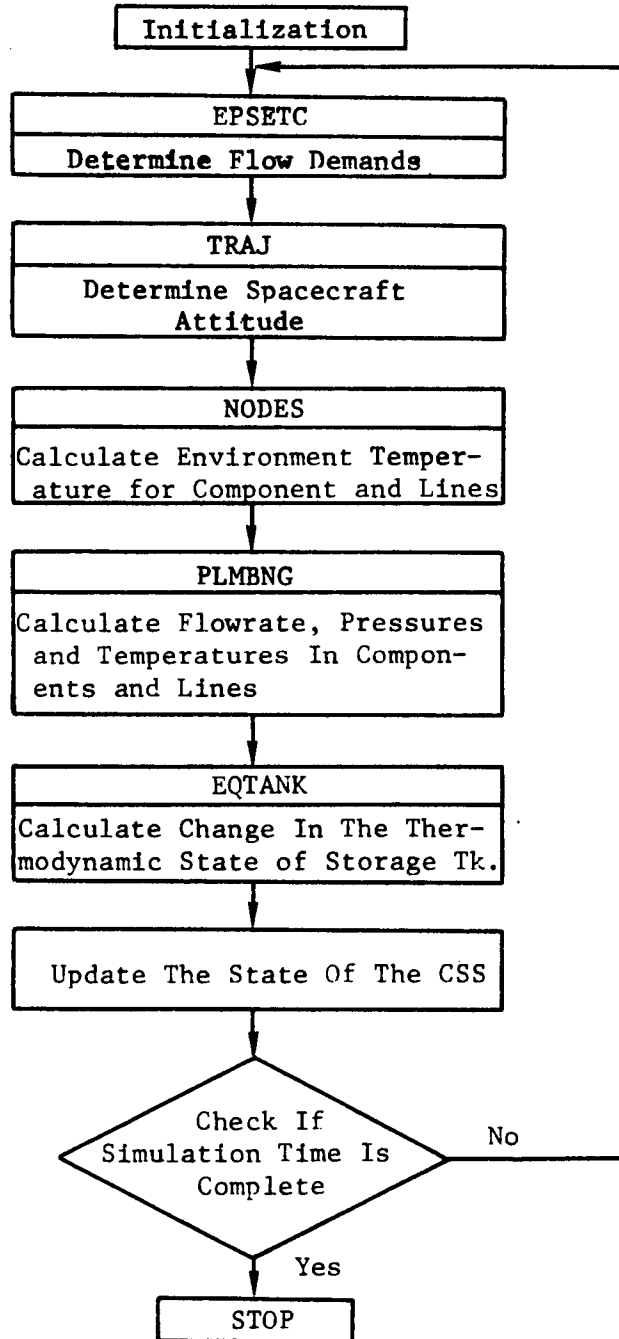


FIGURE 8
STORAGE TANK MODEL
FLOW DIAGRAM

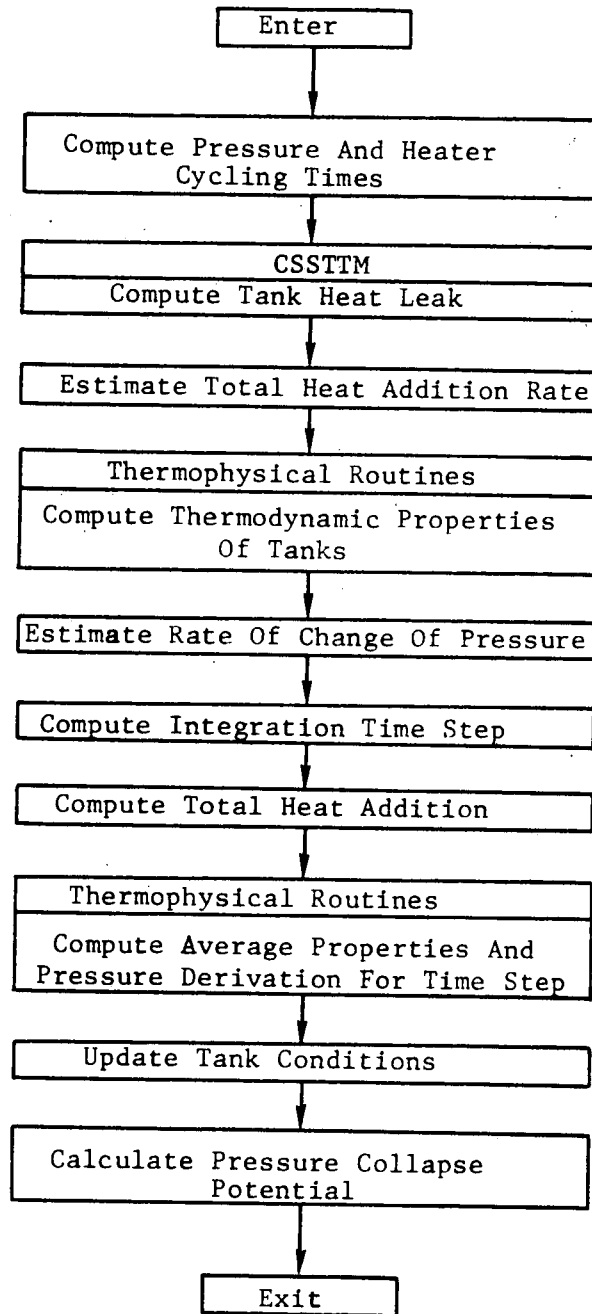


FIGURE 9
OXYGEN TANK NODAL MODEL

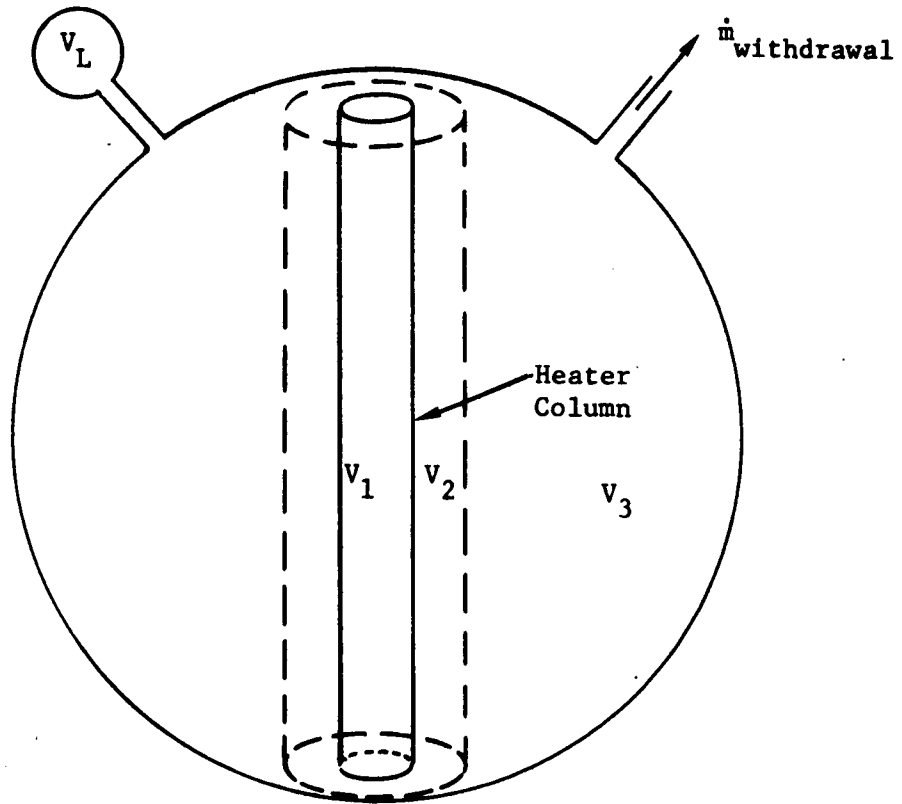


FIGURE 10
J TYPE COMPONENT AND LINES
MODEL FLOW DIAGRAM

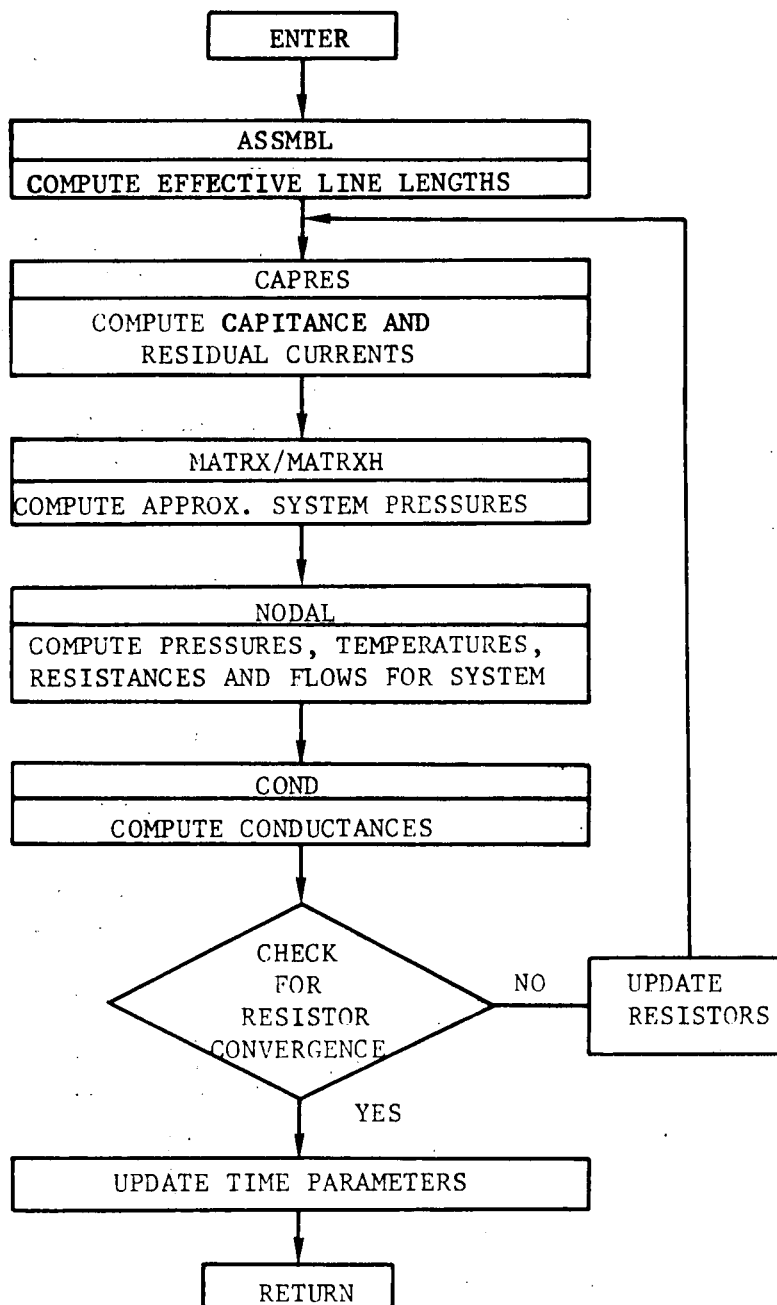
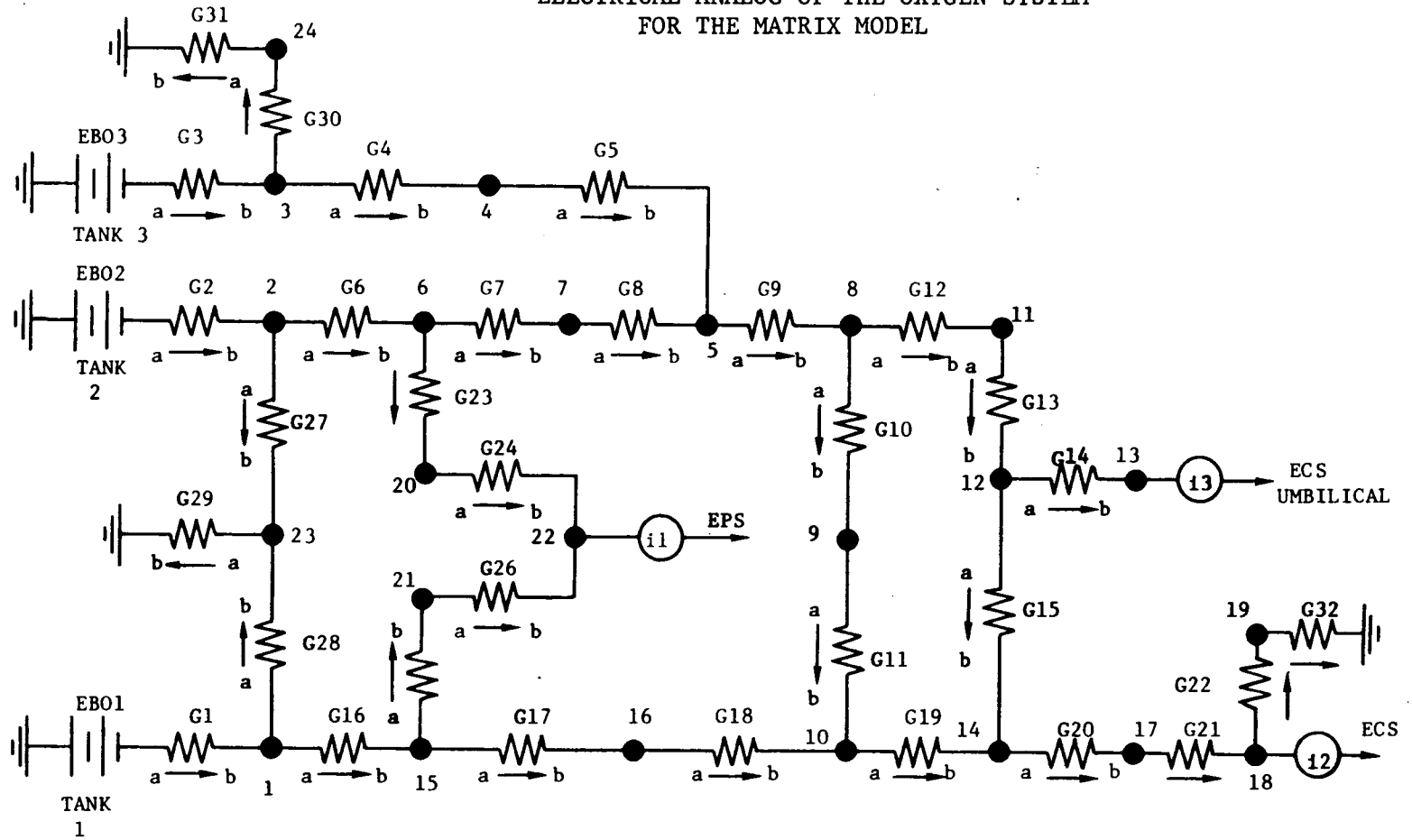


FIGURE 11

ELECTRICAL ANALOG OF THE OXYGEN SYSTEM
FOR THE MATRIX MODEL



378

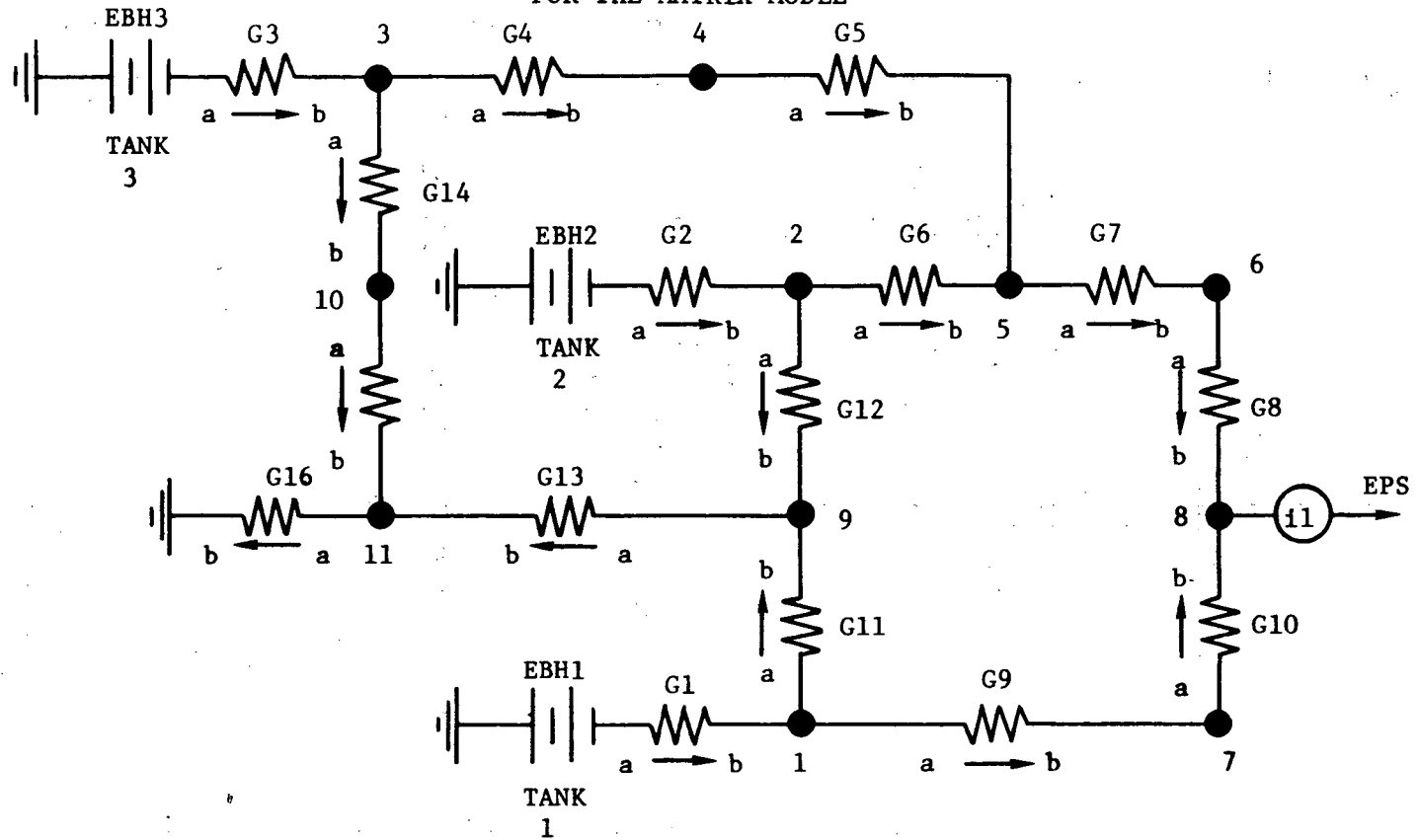
a Upstream
b Downstream

EBOx Electrical Potential Analog
in tanks
Gx Conductance analog

(ix) Flow Demand
● Matrix Nodes

FIGURE 12

ELECTRICAL ANALOG OF THE HYDROGEN SYSTEM
FOR THE MATRIX MODEL



379

a Upstream
b Downstream

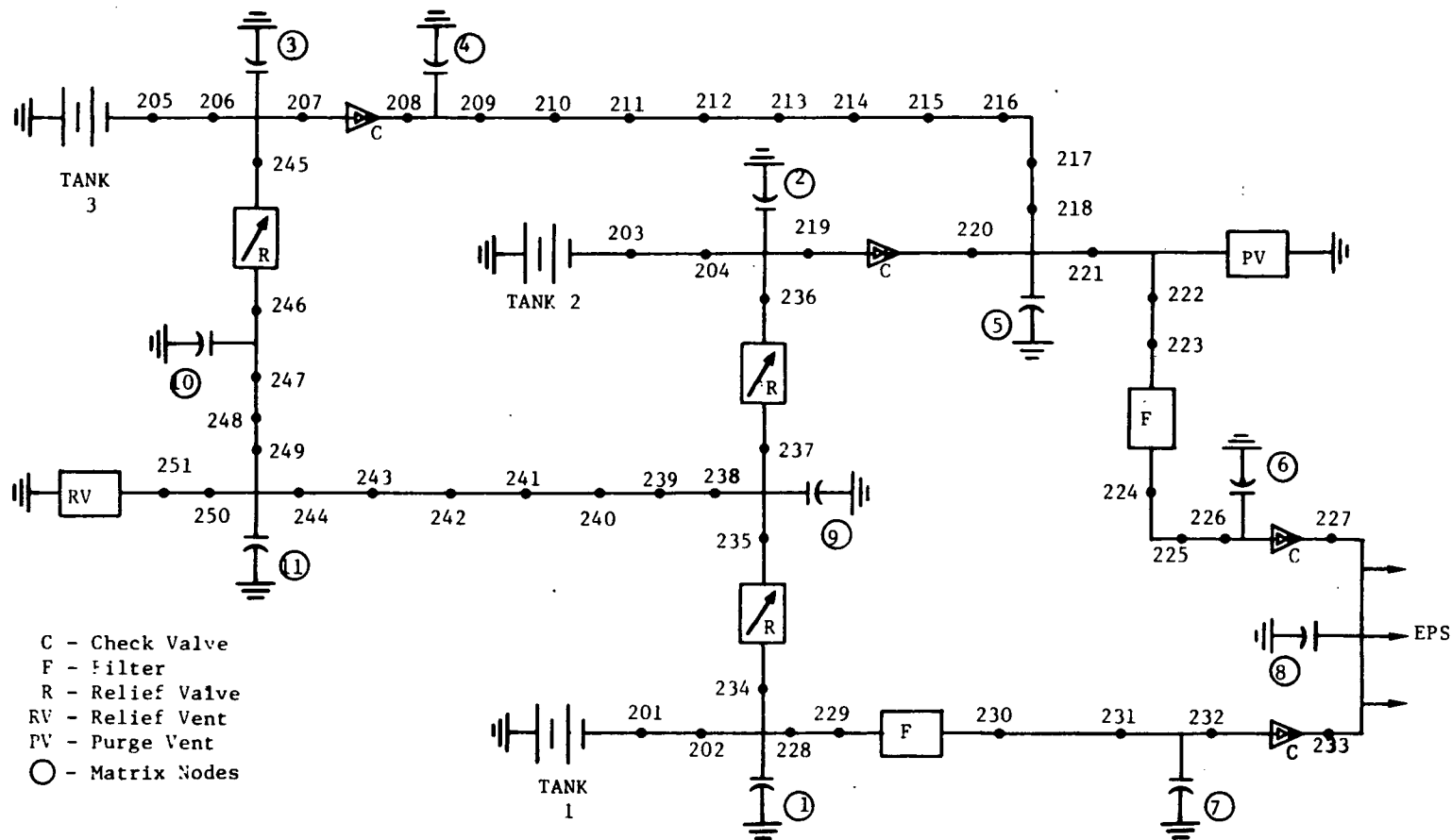
EBH2 Electrical Potential analog for tanks
Gx Conductance Analog

(ix) Flow Demand
● Matrix Nodes

FIGURE 14

ELECTRICAL ANALOG OF THE HYDROGEN SYSTEM FOR THE NODAL MODEL

382



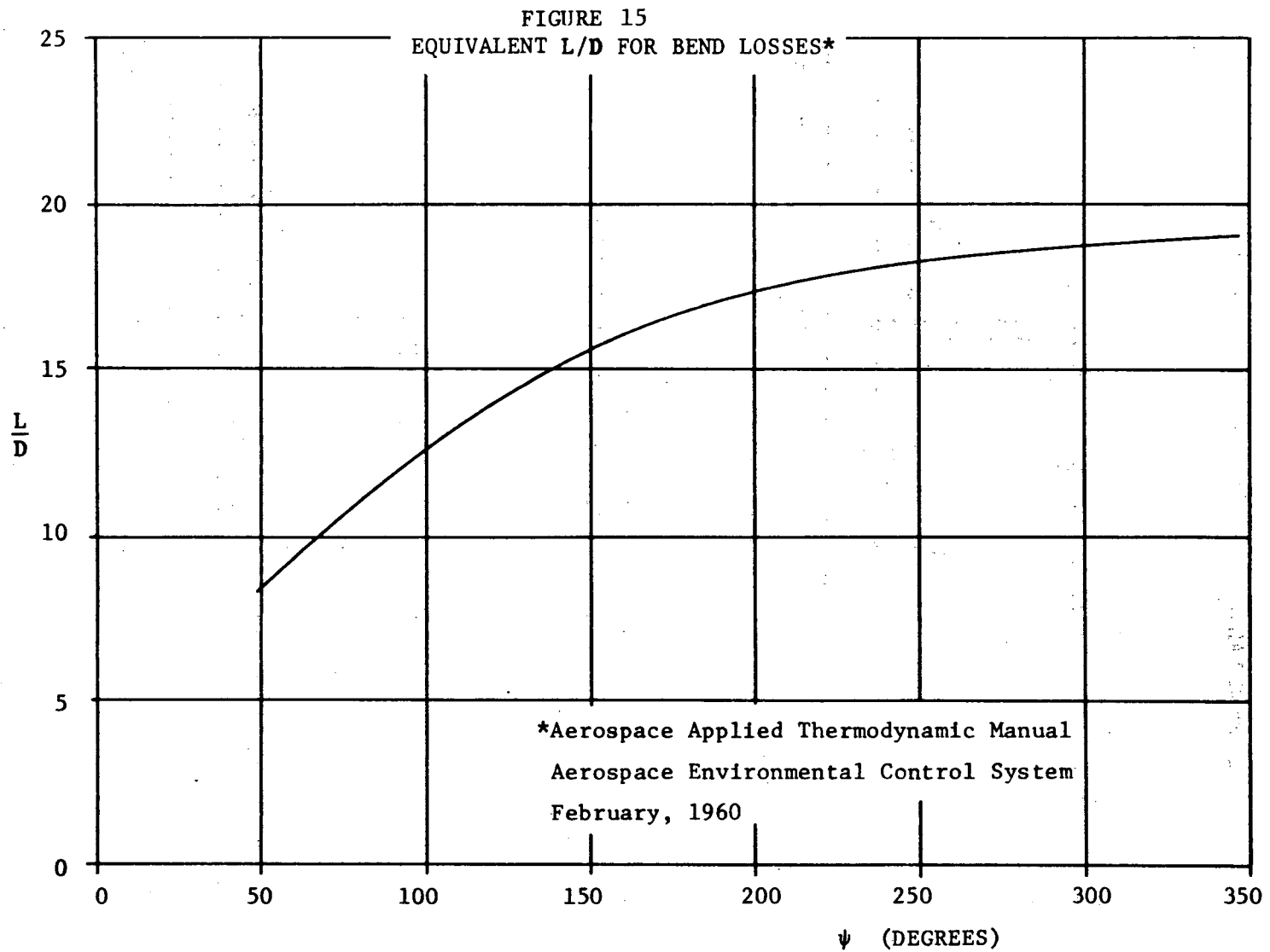


FIGURE 16

CHECK VALVE RESISTANCE CHARACTERISTICS

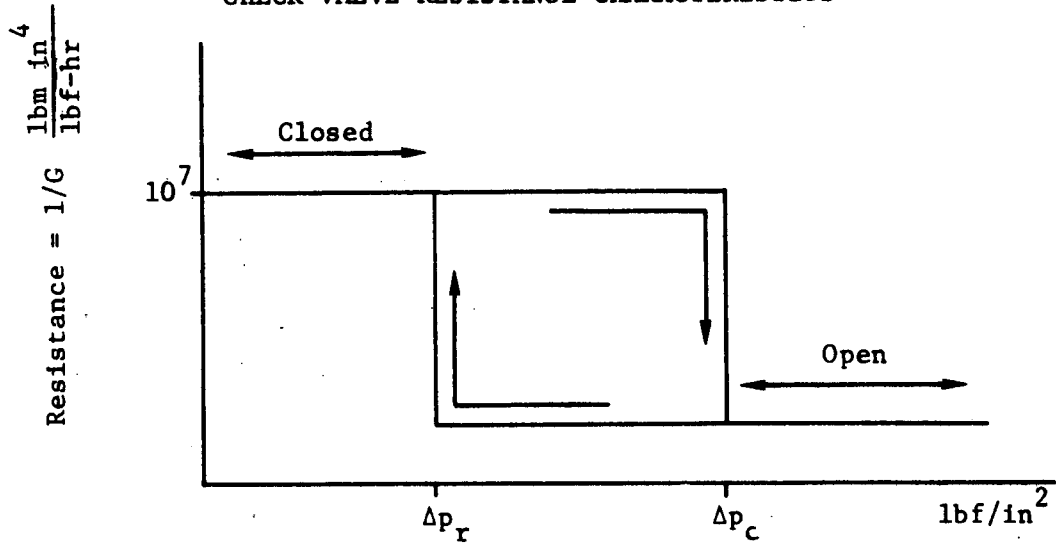


FIGURE 17

RELIEF VALVE RESISTANCE CHARACTERISTICS

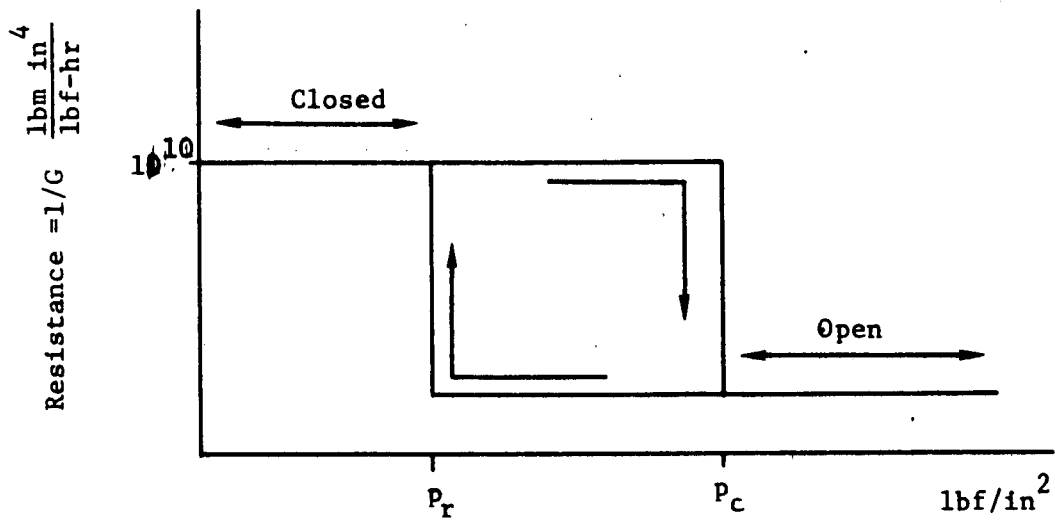


FIGURE 18
 RESTRICTOR PRESSURE DROP*

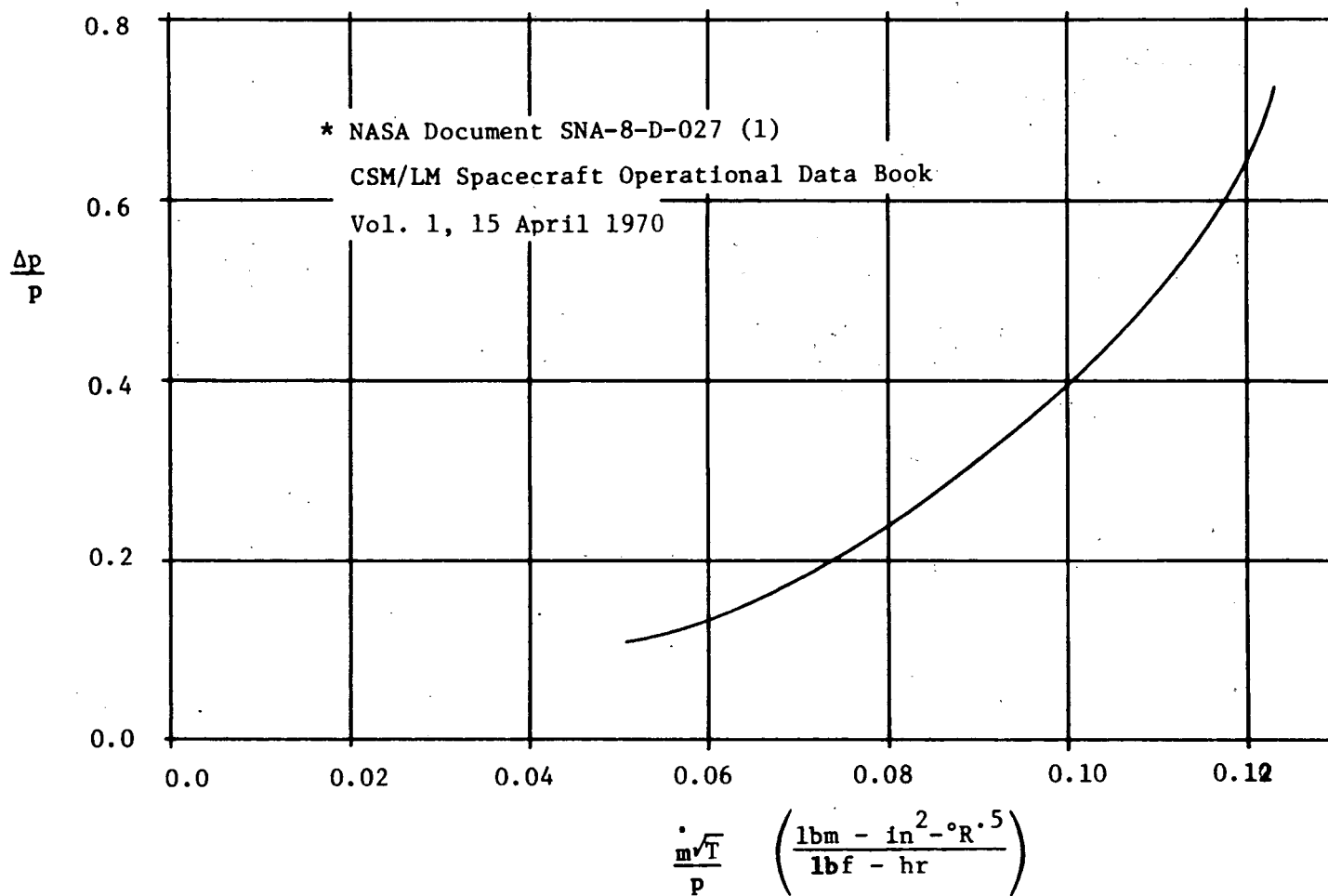
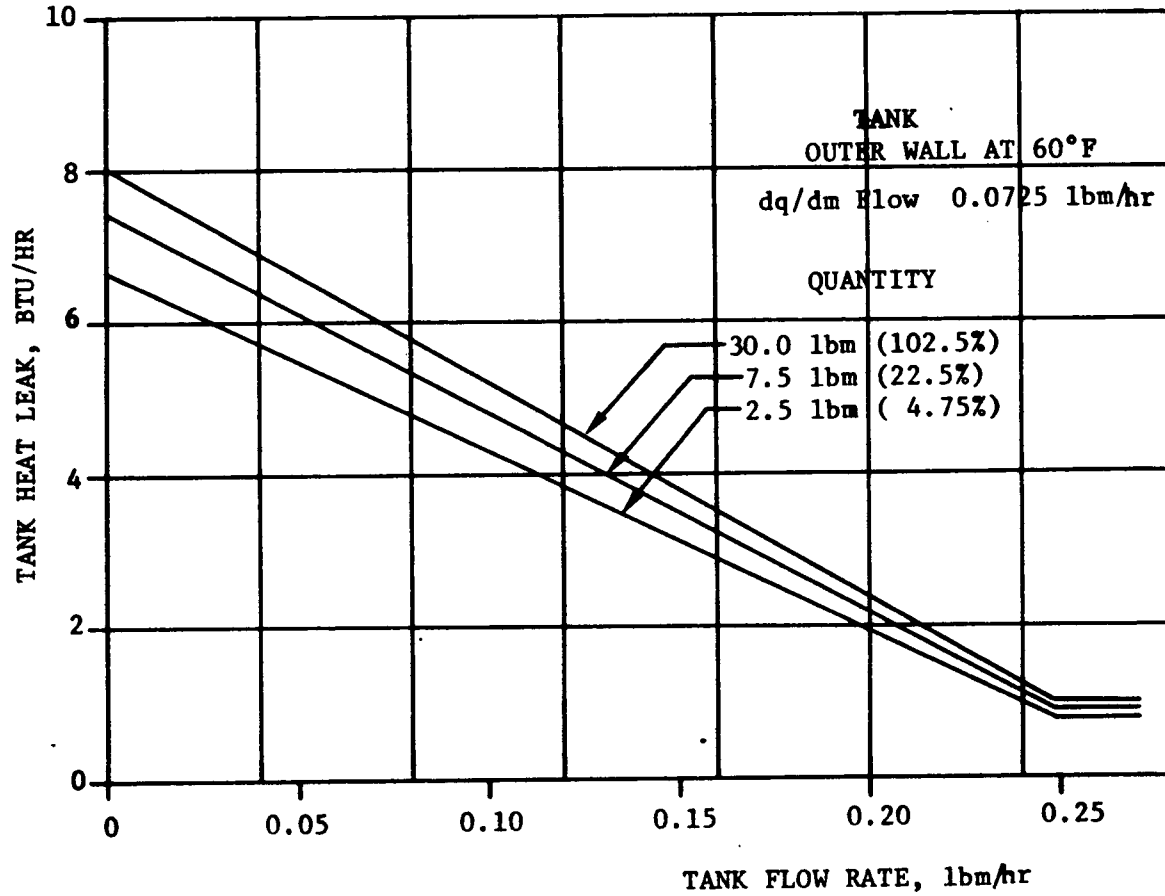


FIGURE 19
HYDROGEN TANK HEAT LEAK



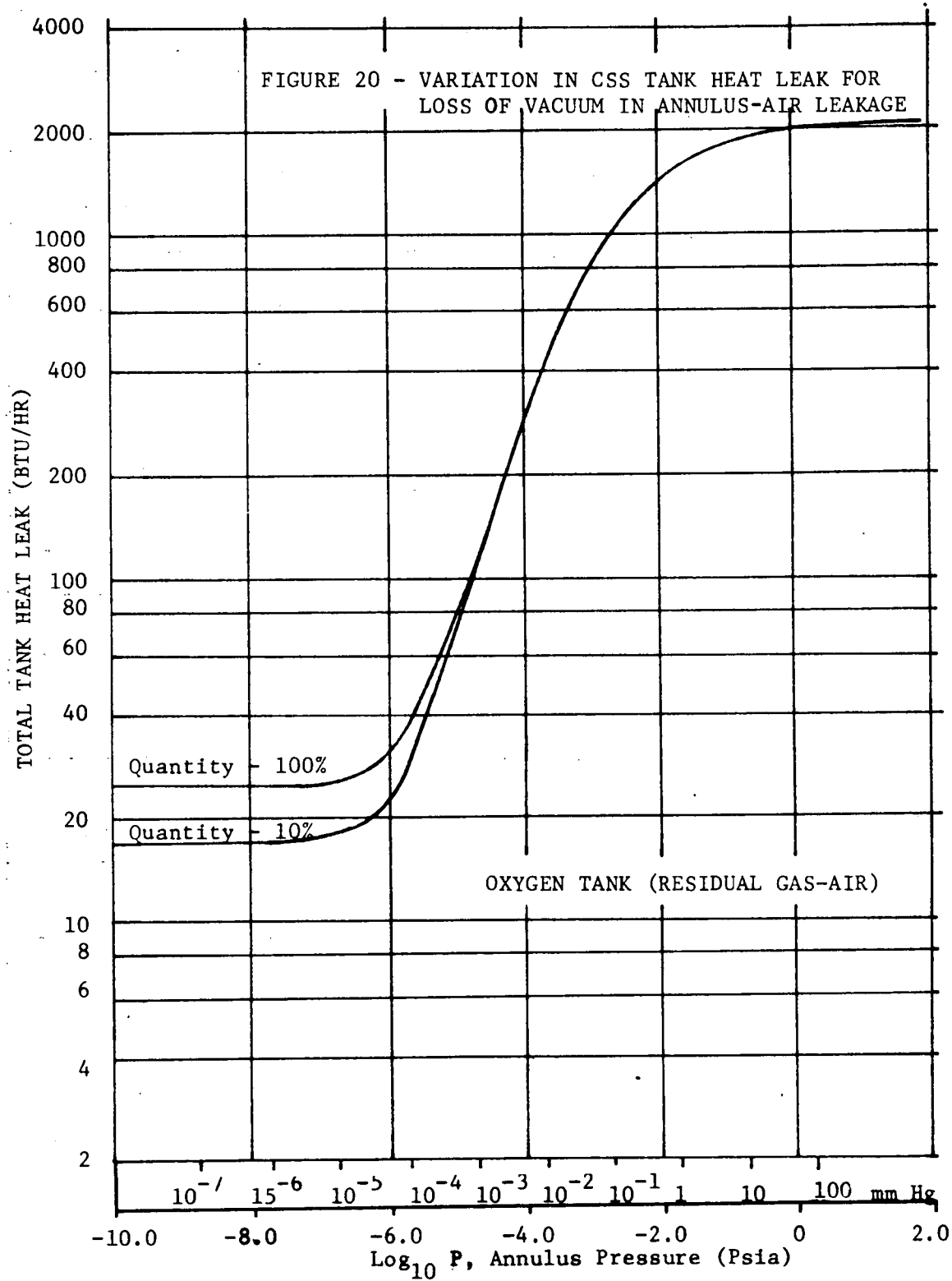
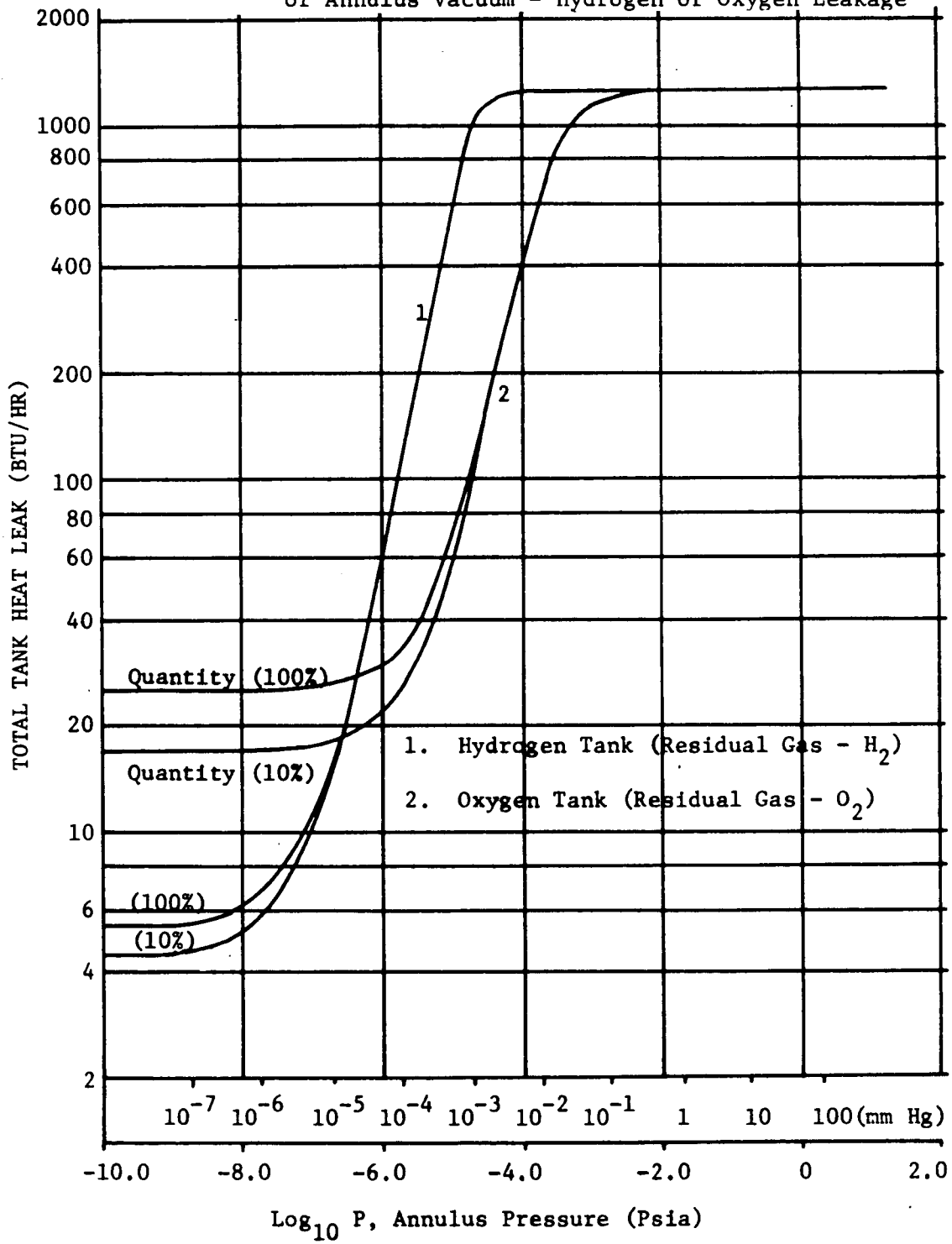


FIGURE 21 - Variation of CSS Tank Heat Leak for Loss of Annulus Vacuum - Hydrogen or Oxygen Leakage



APPENDIX I
NOMENCLATURE

| | |
|------------------|---|
| A | Area, in ² . |
| A _c | Accommodation coefficient, equal to 1.0. |
| C | Capacitance analog, $C = \frac{V}{2RT_p}$, lbm - in ⁴ /lbf ² |
| c _p | Specific heat of fluid at constant pressure, btu/(lbm-°R). |
| c _v | Specific heat of fluid at constant volume, btu/(lbm - °R). |
| d | Wall thickness, in. |
| D | Line diameter, in. |
| E | Electrical potential analog, $E = p^2$, lbf ² /in ⁴ . |
| En | Energy of system |
| f | Friction factor, dimensionless. |
| G | Conductance analog lbf ² -hr/(lbm-in ⁴) |
| g _c | Gravity constant lbm-in/(lbf-hr ²) |
| h | Enthalpy of stored fluid, btu/lbm |
| h' | Enthalpy at initial state, btu/lbm |
| h _{vcs} | Enthalpy of fluid in vapor cooled shroud, btu/lbm. |
| I | Current analog, $I = \dot{m}$, lbm/hr. |
| I _R | Residual current analog, $I_R = \frac{pV}{RT^2} = \frac{dT}{dt}$, lbm/hr. |
| k | Thermal conductivity, btu/(hr-ft-°R). |
| K | Constant, $K = \left(\frac{g_c n}{R}\right)^{1/2} \left(\frac{n+1}{2}\right) - \frac{n+1}{2(n-1)}$, lbm-°R ^{1/2} /(lbf-hr). |
| K _n | Knudsen number, λ/l , dimensionless. |
| l | Characteristic length, ft. |

| | |
|-----------|--|
| L | Length, in. |
| M | Gas molecular weight, lbm/(lb-mole) |
| m | Mass, lbm. |
| \dot{m} | Mass flowrate, lbm/hr. |
| n | Ratio of specific heats, c_p/c_v , dimensionless. |
| N | Polytropic exponent for gas lines attached to tank, dimensionless. |
| N_{RE} | Reynolds number, $\frac{\rho V D}{\mu}$, dimensionless. |
| P, p | Pressure, psia |
| q | Total heat input rate, btu/hr. |
| \dot{q} | Heat leak flux, btu/(hr-ft ²) |
| Q_R | Radiation heat leak, btu/hr. |
| r | Mean pressure vessel radius, in. |
| R | Universal gas constant. |
| R_1 | Inner tank wall radius, ft. |
| R_2 | Outer tank wall radius, ft. |
| s | Fluid velocity, in/hr. |
| t | Time, hr. |
| T | Temperature, °R. |
| T_1 | Temperature of tank outer wall, °R. |
| T_2 | Temperature of tank inner wall, °R. |
| T_{vcs} | Average temperature of fluid in vapor cooled shroud, °R. |
| u | Internal energy of fluid, btu/lbm. |

| | |
|------------|---|
| U | Overall heat transfer coefficient, $\text{btu}/(\text{hr-in}^2\text{-}^\circ\text{R})$. |
| v | Specific volume, ft^3/lbm . |
| V | Tank Volume, ft^3 . |
| V_L | Volume of lines attached to tank, ft^3 . |
| Y | Young's modulus for tank material, psi. |
| α | Tank material thermal expansion coefficient, $1/^\circ\text{R}$. |
| β | Tank thickness, in. |
| Δ | Difference, dimensionless |
| ϵ | Emissivity, dimensionless |
| θ | Thermodynamic function, $-\rho \left. \frac{\partial H}{\partial \rho} \right _p$, btu/lbm . |
| λ | Mean free path, ft. |
| μ | Viscosity, $\text{lbm}/(\text{in-hr})$. |
| ρ | Fluid density, lbm/ft^3 . |
| σ | Stephan-Boltzman constant, $= 1.1 \times 10^{-11}$, $\text{btu}/(\text{hr-in}^2\text{-}^\circ\text{R}^4)$. |
| ν | Poisson's ratio for tank material, dimensionless. |
| ϕ | Thermodynamic function, $\frac{1}{\rho} \left. \frac{\partial p}{\partial u} \right _p$ $\text{psia-ft}^3/\text{btu}$. |
| ψ | Line bend angle, degrees. |

Subscripts

| | |
|----|------------------------|
| c | Cracking |
| i | Inlet |
| j | Outlet |
| k | Arbitrary Line or node |
| l | Arbitrary line or node |
| LM | Logarithmic mean |
| r | Reseat |
| R | Residual |
| s | Sink |

APPENDIX II
DERIVATION OF dp/dt FOR VARIABLE VOLUME TANKS
DUE TO PRESSURE AND TEMPERATURE CHANGES

Introduction.

An expression for the rate of change of pressure for the cryogenic storage tanks has been developed for a constant volume (Reference A-1) and for a variable volume caused by tank stretch due to pressure changes (Reference A-2). The latter expression is:

$$\frac{dp}{dt} = \frac{\frac{\phi\theta}{V} \dot{m} + \frac{\phi}{V} q}{1 + \frac{3\phi\phi\rho r}{2dY} (1-\nu)} \quad (\text{AII-1})$$

where:

$$\theta = -\rho \left(\frac{\partial h}{\partial \rho} \right)_p \quad (\text{AII-2})$$

$$\phi = \frac{1}{\rho} \left(\frac{\partial p}{\partial u} \right)_\rho \quad (\text{AII-3})$$

If Young's Modulus, Y, is taken as infinity (no tank stretch), Equation (AII-1) reduces to the expression for dp/dt as presented in Reference A-1.

The expression for dp/dt considering variable volume resulting from tank stretch due to both pressure and temperature changes is developed in this Appendix. For completeness, a portion of the derivation from Reference A-2 is also presented.

Derivation.

The First Law of Thermodynamics may be written:

$$\frac{dE_n}{dt} = q + \dot{m} h' - p \frac{dV}{dt}$$

If it is assumed that the system is at uniform pressure, p, and that kinetic and potential energy may be neglected, then

$$E_n = mu = \rho Vu$$

and

$$\frac{d(\rho V u)}{dt} = q + \dot{m} h' - p \frac{dV}{dt}$$

$$\frac{ud(\rho V)}{dt} + \rho V \frac{du}{dt} = q + \dot{m} h' - p \frac{d(mv)}{dt}$$

Now

$$u = h - pv.$$

Then

$$\frac{udm}{dt} + \rho V \frac{d(h-pv)}{dt} = q + \dot{m} h' - \frac{pmdv}{dt} - \frac{pvdm}{dt}$$

$$\dot{m} u + \rho V \frac{dh}{dt} - \rho V \frac{d(pv)}{dt} = q + \dot{m} h' - pm \frac{dv}{dt} - p v \dot{m}$$

$$\dot{m} (u + pv) + \rho V \frac{dh}{dt} - \rho V p \frac{dv}{dt} - \rho V v \frac{dp}{dt} = q + \dot{m} h' - pm \frac{dv}{dt}$$

$$\dot{m} h + \rho V \frac{dh}{dt} - \cancel{m p \frac{dv}{dt}} - V \frac{dp}{dt} = q + \dot{m} h' - \cancel{p m \frac{dv}{dt}}$$

$$V \frac{dp}{dt} = \rho V \frac{dh}{dt} - q + \dot{m} (h - h')$$

$$\frac{dp}{dt} = \rho \frac{dh}{dt} - \frac{q}{V} + \frac{\dot{m}}{V} (h - h').$$

Since $h \approx h'$, the last term is negligible.

$$\text{Thus, } \frac{dp}{dt} = \rho \frac{dh}{dt} - \frac{q}{V}$$

(AII-4)

Assume that

$$h = h(p, \rho).$$

then

$$dh = \left. \frac{\partial h}{\partial p} \right|_{\rho} dp + \left. \frac{\partial h}{\partial \rho} \right|_{p} d\rho$$

$$\frac{dh}{dt} = \left. \frac{\partial h}{\partial p} \right|_{\rho} \frac{dp}{dt} + \left. \frac{\partial h}{\partial \rho} \right|_p \frac{d\rho}{dt}.$$

Now,

$$V = \frac{m}{\rho}$$

and
$$\frac{d\rho}{dt} = \frac{d\left(\frac{m}{V}\right)}{dt} = \frac{1}{V} \frac{dm}{dt} - \frac{m}{V^2} \frac{dV}{dt} = \frac{\rho}{m} \frac{dm}{dt} - \frac{\rho}{V} \frac{dV}{dt}.$$

So,

$$\frac{dh}{dt} = \left. \frac{\partial h}{\partial p} \right|_{\rho} \frac{dp}{dt} + \left. \frac{\partial h}{\partial \rho} \right|_p \left[\frac{\rho}{m} \frac{dm}{dt} - \frac{\rho}{V} \frac{dV}{dt} \right].$$

Substituting for Θ from Equation (AII-2)

$$\frac{dh}{dt} = \left. \frac{\partial h}{\partial p} \right|_{\rho} \frac{dp}{dt} - \frac{\Theta}{m} \dot{m} + \frac{\Theta}{V} \frac{dV}{dt}$$

Since $h = u + pv = u + \frac{p}{\rho},$

then
$$\left. \frac{\partial h}{\partial p} \right|_{\rho} = \left. \frac{\partial u}{\partial p} \right|_{\rho} + \left. \frac{\partial \left(\frac{p}{\rho}\right)}{\partial p} \right|_{\rho}$$

$$\left. \frac{\partial h}{\partial p} \right|_{\rho} = \left. \frac{\partial u}{\partial p} \right|_{\rho} + \frac{1}{\rho}$$

So,

$$\frac{dh}{dt} = \left[\left. \frac{\partial u}{\partial p} \right|_{\rho} + \frac{1}{\rho} \right] \frac{dp}{dt} - \frac{\Theta}{m} \dot{m} + \frac{\Theta}{V} \frac{dV}{dt}.$$

Substituting for Θ from Equation (AII-3)

$$\frac{dh}{dt} = \left[\frac{1}{\rho\phi} + \frac{1}{\rho} \right] \frac{dp}{dt} - \frac{\Theta}{m} \dot{m} + \frac{\Theta}{V} \frac{dV}{dt}.$$

(AII-5)

It is at this point that the assumption is made that tank stretch is a function of both pressure, p , and temperature, T .

$$\frac{dV}{dt} = \left. \frac{\partial V}{\partial p} \right|_T \frac{dp}{dt} + \left. \frac{\partial V}{\partial T} \right|_p \frac{dT}{dt} . \quad (\text{AII-6})$$

It is necessary to determine dT/dt

$$\frac{dT}{dt} = \left. \frac{\partial T}{\partial p} \right|_\rho \frac{dp}{dt} + \left. \frac{\partial T}{\partial \rho} \right|_p \frac{d\rho}{dt} . \quad (\text{AII-7})$$

Now, $m = \rho V$

$$\frac{dm}{dt} = \frac{d\rho}{dt} V + \rho \frac{dV}{dt}$$

$$\text{So, } \frac{d\rho}{dt} = \frac{\dot{m}}{V} - \frac{\rho}{V} \frac{dV}{dt} \quad (\text{AII-8})$$

Substituting Equations (AII-8) into Equation (AII-7), and substituting Equation (AII-7) into Equation (AII-6) results in:

$$\frac{dV}{dt} = \left. \frac{\partial V}{\partial p} \right|_T \frac{dp}{dt} + \left. \frac{\partial V}{\partial T} \right|_\rho \left[\left. \frac{\partial T}{\partial p} \right|_\rho \frac{dp}{dt} + \left. \frac{\partial T}{\partial \rho} \right|_p \left(\frac{\dot{m}}{V} - \frac{\rho}{V} \frac{dV}{dt} \right) \right]$$

For convenience, the following substitutions have been made:

$$A = \left. \frac{\partial V}{\partial p} \right|_T \quad B = \left. \frac{\partial V}{\partial T} \right|_p$$

$$C = \left. \frac{\partial T}{\partial p} \right|_\rho \quad D = \left. \frac{\partial T}{\partial \rho} \right|_p$$

Then,

$$\frac{dV}{dt} = A \frac{dp}{dt} + B \left[C \frac{dp}{dt} + D \left(\frac{\dot{m}}{V} - \frac{\rho}{V} \frac{dV}{dt} \right) \right]$$

$$\frac{dV}{dt} = (A + BC) \frac{dp}{dt} + BD \frac{\dot{m}}{V} - \frac{BD\rho}{V} \frac{dV}{dt}$$

$$\left(1 + \frac{BD\rho}{V}\right) \frac{dV}{dt} = (A + BC) \frac{dp}{dt} + \frac{BD\dot{m}}{V}$$

$$\frac{dV}{dt} = \frac{(A + BC) \frac{dp}{dt} + \frac{BD\dot{m}}{V}}{1 + \frac{BD\rho}{V}} \quad (\text{AII-9})$$

Substituting Equation (AII-9) into Equation (AII-5):

$$\frac{dh}{dt} = \left[\frac{1}{\rho\phi} + \frac{1}{\rho} \right] \frac{dp}{dt} - \frac{\Theta}{m} \dot{m} + \frac{\Theta}{V} \left[\frac{(A + BC) \frac{dp}{dt} + \frac{BD\dot{m}}{V}}{1 + \frac{BD\rho}{V}} \right]$$

$$\frac{dh}{dt} = \left[\frac{1}{\rho\phi} + \frac{1}{\rho} + \frac{\Theta(A + BC)}{V + BD\rho} \right] \frac{dp}{dt} - \frac{\Theta\dot{m}}{m} + \frac{\Theta BD\dot{m}}{V(V + BD\rho)}$$

But from Equation (AII-4)

$$\frac{dh}{dt} = \frac{1}{\rho} \frac{dp}{dt} + \frac{q}{\rho V}$$

Therefore,

$$\cancel{\frac{1}{\rho}} \frac{dp}{dt} + \frac{q}{\rho V} = \left[\frac{1}{\rho\phi} + \cancel{\frac{1}{\rho}} + \frac{\Theta(A + BC)}{V + BD\rho} \right] \frac{dp}{dt} - \frac{\Theta\dot{m}}{m} + \frac{\Theta BD\dot{m}}{V(V + BD\rho)}$$

and,

$$\left[\frac{1}{\rho\phi} + \frac{\Theta(A + BC)}{V + BD\rho} \right] \frac{dp}{dt} = \frac{\Theta\dot{m}}{m} - \frac{\Theta BD\dot{m}}{V(V + BD\rho)} + \frac{q}{\rho V}$$

resulting in:

$$\frac{dp}{dt} = \frac{\frac{\Theta\dot{m}}{\rho V} + \frac{q}{\rho V} - \frac{\Theta BD\dot{m}}{V(V + BD\rho)}}{\frac{1}{\rho\phi} + \frac{\Theta(A + BC)}{V + BD\rho}}$$

or,

$$\frac{dp}{dt} = \frac{\frac{\Theta m \dot{\phi}}{V} + \frac{\phi \dot{q}}{V} - \frac{\Theta \phi B D m \dot{\rho}}{V(V+BD\rho)}}{1 + \frac{\phi \Theta \rho (A+BC)}{V+BD\rho}}$$

Substituting for A, B, C and D

$$\frac{dp}{dt} = \frac{\frac{\Theta m \dot{\phi}}{V} + \frac{\phi \dot{q}}{V} - \frac{\Theta \phi m \rho \left. \frac{\partial V}{\partial T} \right|_p \left. \frac{\partial T}{\partial \rho} \right|_p}{1 + \frac{\Theta \phi \rho \left(\left. \frac{\partial V}{\partial p} \right|_T + \left. \frac{\partial V}{\partial T} \right|_p \left. \frac{\partial T}{\partial p} \right|_p \right)} \cdot \frac{V(V + \rho \left. \frac{\partial V}{\partial T} \right|_p \left. \frac{\partial T}{\partial \rho} \right|_p)}{V + \rho \left. \frac{\partial V}{\partial T} \right|_p \left. \frac{\partial T}{\partial \rho} \right|_p} \quad (\text{AII-10})$$

Reference A-2 presents the derivation for change in volume with respect to pressure at constant temperature as:

$$\left. \frac{\partial V}{\partial p} \right|_T = \frac{3rV}{2dY} (1-u) \quad (\text{AII-11})$$

The change in volume with respect to temperature may be obtained as follows:

$$\begin{aligned} \left. \frac{\partial V}{\partial T} \right|_p &= \left. \frac{\partial V}{\partial r} \right|_p \left. \frac{\partial r}{\partial T} \right|_p \\ \left. \frac{\partial V}{\partial r} \right|_p &= \frac{\partial}{\partial r} \left(\frac{4}{3} \pi r^3 \right) = 4 \pi r^2 = \frac{3V}{r} \end{aligned}$$

For small changes in temperature, then

$$\left. \frac{\partial V}{\partial T} \right|_p = \frac{3V}{r} \frac{\Delta r}{\Delta T} = 3\alpha V \quad (\text{AII-12})$$

Substituting these expressions into Equation (AII-10) results in:

$$\frac{\dot{\phi}_m}{V} + \frac{\dot{\phi}_g}{V} = \frac{\theta \dot{\phi}_m \quad 3\alpha\rho \left. \frac{\partial T}{\partial \rho} \right|_p}{V \left(1 + 3\alpha \left. \frac{\partial T}{\partial \rho} \right|_p \right)} \quad (\text{AII-13})$$

$$\frac{dp}{dt} = \frac{1 + \theta \phi \rho \left(\frac{3r}{2dY} (1 - \nu) + 3\alpha \left. \frac{\partial T}{\partial p} \right|_\rho \right)}{1 + 3\alpha \rho \left. \frac{\partial T}{\partial \rho} \right|_p}$$

It is necessary to account for one additional effect which results in a variation in the change in volume with respect to pressure. This effect is the compression of the fluid in the fill and vent lines of the tank. These lines extend from the pressure vessel to the warm environment. The fluid at the cold ends is relatively incompressible as compared to the near ideal gas conditions at the other ends. When pressure increases, the fluid in the lines is compressed by the expanding stored fluid which move up the lines. To account for this effect, it was assumed that the lines will be filled with an ideal gas at ambient temperature and that no mixing between the tanked cryogen and the perfect gas would take place. Then:

$$pV_L^n = \text{constant.}$$

Thus,

$$V_L^n \frac{dp}{dt} + npV_L^{n-1} \frac{dV_L}{dt} = 0$$

or

$$\frac{dV_L}{dt} = \frac{-V_L}{np} \frac{dp}{dt} \quad (\text{AII-14})$$

The mass flow, \dot{m} , is the total flow from the tank:

$$\dot{m} = \dot{m}_0 + \dot{m}_2 \quad (\text{AII-15})$$

where: \dot{m}_0 = flow to EPS and ECS subsystems, lbm/hr.

$$\dot{m}_2 = \rho \frac{dV_L}{dt} = \text{flow from fill and vent lines, lbm/hr}$$

Note: Flow out of the tank is negative in sign.

Substituting Equation (AII-14) into Equation (AII-15) yields:

$$\dot{m} = \dot{m}_o - \rho \frac{V_L}{np} \frac{dp}{dt}$$

When this equation is substituted into equation (AII-13) and rearranged, the resulting expression is:

$$\frac{\partial \phi}{\partial V} \dot{m}_o + \frac{\phi}{V} \dot{q} - \frac{\partial \phi}{\partial V} \frac{\dot{m}_o 3\alpha\rho \left. \frac{\partial T}{\partial \rho} \right|_p}{(1 + \rho 3\alpha \left. \frac{\partial T}{\partial \rho} \right|_p)} \tag{AII-16}$$

$$\frac{dp}{dt} = \frac{1 + \frac{\partial \phi}{\partial V} \frac{\rho V_L}{np} - \frac{\partial \phi}{\partial V} \frac{V_L 3\alpha\rho^2 \left. \frac{\partial T}{\partial \rho} \right|_p}{np (1 + 3\alpha\rho \left. \frac{\partial T}{\partial \rho} \right|_p)} + F$$

where:

$$F = \frac{\partial \phi \rho \left(\frac{3r}{2dY} (1-u) + 3\alpha \left. \frac{\partial T}{\partial \rho} \right|_p \right)}{1 + 3\alpha\rho \left. \frac{\partial T}{\partial \rho} \right|_p}$$

Thus, Equation (AII-16) describes the rate of change of pressure for a variable tank volume considering both pressure and temperature changes. Note that if the coefficient of thermal expansion, α , is equal to zero and if the plumbing fluid compression volume, V_L , is zero, Equation (AII-1) is obtained. Table A-1 presents the constants used for both the oxygen and hydrogen tanks. The partial derivatives are obtained by differentiating the equation of state. Since the Integrated Systems Program uses an equation of state that is a function of temperature and density, it is desirable to obtain $\partial T/\partial \rho$ in the following form:

$$\left. \frac{\partial T}{\partial \rho} \right|_p \left. \frac{\partial \rho}{\partial p} \right|_T \left. \frac{\partial p}{\partial T} \right|_\rho = -1$$

This relation was taken from Reference A-4, page 32, Equation (3-11).

Then

$$\left. \frac{\partial T}{\partial \rho} \right|_p = \frac{1}{-\left. \frac{\partial \rho}{\partial p} \right|_T \left. \frac{\partial p}{\partial T} \right|_\rho} = - \left. \frac{\partial p}{\partial \rho} \right|_T \left. \frac{\partial T}{\partial p} \right|_\rho$$

Thus, this partial derivative may also be obtained from the equation of state.

TABLE A-1
CRYOGENIC TANK PROPERTIES

OXYGEN

| | |
|---|-------------------------|
| Material..... | Inconel 718 |
| Volume, V, ft ³ | 4.75 |
| Inside Radius, r, in..... | 12.513 |
| Young's Modulus, Y, psi..... | 30 x 10 ⁶ |
| Poisson's Ratio, ν , dimensionless..... | 0.29 |
| Wall Thickness, d, in..... | 0.059 |
| Coefficient of Thermal Expansion, α , /°R..... | 5.93 x 10 ⁻⁶ |

HYDROGEN

| | |
|---|-------------------------|
| Material..... | Titanium-5AL-2.5SN ELI |
| Volume, V, ft ³ | 6.80 |
| Inside Radius, r, in..... | 14.103 |
| Young's Modulus, Y, psi..... | 17 x 10 ⁶ |
| Poisson's Ratio, ν , dimensionless..... | 0.30 |
| Wall Thickness, d, in..... | 0.044 |
| Coefficient of Thermal Expansion, α , /°R..... | 1.23 x 10 ⁻⁶ |

Note: Values for α were derived from Reference A-3, Table 7.3.4, page 7-59.

APPENDIX II REFERENCES

- A-1. TRW IOC 70.4354.3-84, "Thermodynamics Relations for the Quasi-Static Flow of Single Phase Fluids," C. E. Barton, 17 August 1970.
- A-2. TRW IOC 70.4354.36-2, "Derivation of the Cryogenic Pressure Rise/Decay Rates," C. W. Wurst, 26 October 1970.
- A-3. "Apollo Fuel Cell and Cryogenic Gas Storage System Flight Support Handbook," NASA/MSC, 18 February 1970.
- A-4. Thermodynamics, the Kinetic Theory of Gases, and Statistical Mechanics, F. W. Sears, Addison-Wesley Publishing, 1953.

APPENDIX III
DERIVATION OF EQUATIONS USED IN THE
COMPONENT AND LINE MODEL

MATRIX MODEL

The matrix model determines the pressures for each of the oxygen and hydrogen system nodes shown in Figures 11 and 12, respectively.

The conservation of mass principle may be written:

$$\sum \dot{m} = V \frac{d\rho}{dt} \quad (\text{AIII-1})$$

For a perfect gas,

$$p = \rho RT. \quad (\text{AIII-2})$$

Combining Equations (AIII-1) and (AIII-2) and performing the differentiation results in:

$$\sum \dot{m} = \frac{V}{RT^2} \left(T \frac{dp}{dt} - p \frac{dT}{dt} \right). \quad (\text{AIII-3})$$

To set up an electrical analogy, let

$$E \equiv p^2 \quad (\text{AIII-4})$$

for an equivalent driving function, and

$$I \equiv \dot{m} \quad (\text{AIII-5})$$

for the current.

In terms of the transforms variables, Equation (AIII-3) becomes:

$$\sum I = \frac{V}{2RT\sqrt{E}} \frac{dE}{dt} - \frac{V\sqrt{E}}{RT^2} \frac{dT}{dt} \quad (\text{AIII-6})$$

or

$$\sum I = C \frac{dE}{dt} - I_R \quad (\text{AIII-7})$$

where

$$C = \frac{V}{2RT\sqrt{E}} \quad (\text{AIII-8})$$

is an equivalent capacitance, and

$$I_R = \frac{V\sqrt{E}}{RT^2} \frac{dT}{dt} \quad (\text{AIII-9})$$

is an equivalent residual current.

NODAL MODEL

The nodal model determines the pressures of the oxygen and hydrogen along each leg of the oxygen and hydrogen, Figures 13 and 14, respectively.

The instantaneous pressure drop for incompressible flow through a line with inlet i and outlet j is given by the Darcy-Weisbach equation,

$$p_i - p_j = \left(\frac{4fL}{D}\right)_{ij} \frac{\rho s^2}{2g_c} \quad (\text{AIII-10})$$

For incompressible flow in a circular tube,

$$\dot{m} = \rho A s = \frac{\pi D^2 \rho s}{4} \quad (\text{AIII-11})$$

Combining Equations (AIII-10) and (AIII-11) and simplifying results in:

$$p_i - p_j = \left(\frac{4fL}{D}\right)_{ij} \frac{8\dot{m}^2}{g_c \pi^2 D^4 \rho} \quad (\text{AIII-12})$$

Let the mean density between i and j be based on the average pressure and temperature. Then,

$$\rho_{ij} = \frac{1}{R} \frac{p_i + p_j}{T_i + T_j} \quad (\text{AIII-13})$$

Substituting Equation (AIII-13) into Equation (AIII-12) and simplifying yields:

$$p_i^2 - p_j^2 = \left[\frac{8R(T_i + T_j)}{g_c \pi^2 D^4} \left(\frac{4fL}{D}\right)_{ij} \right] \dot{m}^2 \quad (\text{AIII-14})$$

For laminar, incompressible flow in a circular tube,

$$f = \frac{16}{N_{RE}} = \frac{4\pi\mu D}{\dot{m}} \quad (\text{AIII-15})$$

Combining Equations (AIII-14) and (AIII-15) and simplifying results in:

$$p_i^2 - p_j^2 = \left[\frac{128L\mu R}{g_c \pi D^4} (T_i + T_j) \right] \dot{m} \quad (\text{AIII-16})$$

In terms of the electrical analog variables, Equation (AIII-16) becomes:

$$E_i - E_j = \frac{I}{G} \quad (\text{AIII-17})$$

where

$$G = \left[\frac{128L\mu R}{g_c \pi D^4} (T_i + T_j) \right]^{-1} \quad (\text{AIII-18})$$

An instantaneous heat balance through a line with inlet i and outlet j is:

$$UA \Delta T_{LM} = \dot{m} c_p (T_j - T_i) \quad (\text{AIII-19})$$

where

$$\Delta T_{LM} = \frac{(T_k - T_i) - (T_k - T_j)}{\ln \left(\frac{T_k - T_i}{T_k - T_j} \right)} \quad (\text{AIII-20})$$

Combining Equations (AIII-19) and (AIII-20) and simplifying yields:

$$T_j = \left[1 - e^{-\left(\frac{UA}{\dot{m}c_p} \right)} \right] T_k + e^{-\left(\frac{UA}{\dot{m}c_p} \right)} T_i \quad (\text{AIII-21})$$